Progress in Retinal and Eye Research 73 (2019) 100765

Contents lists available at ScienceDirect

Progress in Retinal and Eye Research

journal homepage: www.elsevier.com/locate/preteyeres

Visual loss and recovery in chiasmal compression

Helen V. Danesh-Meyer[a,1,*], Jinny J. Yoon[a,1], Mitchell Lawlor[b,1], Peter J. Savino[c,1]

[a] Department of Ophthalmology, University of Auckland, Private Bag 92019, Auckland, 1142, New Zealand
[b] Save Sight Institute, Discipline of Ophthalmology, Faculty of Medicine and Health, University of Sydney, NSW, Australia
[c] Shiley Eye Institute, The Viterbi Family Department of Ophthalmology, University of California, San Diego, USA

ARTICLE INFO

Keywords:
Optic chiasm
Optic nerve compression
Pituitary adenoma
Meningioma
Retinal ganglion cells
Axonal injury
Visual pathways
Visual prognosis
Optical coherence tomography

ABSTRACT

Compression of the optic chiasm causes an optic neuropathy that may be associated with reversible visual loss often immediately following surgical decompression. While the precise pathogenesis of retinal ganglion cell impairment and eventual death remains poorly understood, a number of putative mechanisms may play a role. In this article we review the evidence supporting various stages of visual loss and recovery in chiasmal compression. These include conduction block, demyelination, ischemic insult, and retrograde and anterograde degeneration. We also describe novel advances in magnetic resonance imaging with specialized modalities such as diffusion tensor imaging have provided further information to explain the underlying mechanism of visual loss. Functional measures including electrophysiology are time-consuming but have shown moderate prognostic ability. Optical coherence tomography has provided novel new biomarkers for predicting outcome following surgical decompression. Both retinal nerve fiber layer thickness and ganglion cell complex thicknesses have shown to have excellent predictive power. Such advances serve to inform patients and clinicians of pre-operative factors that predict the extent of visual recovery following medical or surgical treatment of para-chiasmal lesions.

1. Introduction

The optic chiasm is a critical juncture for the visual sensory system and anatomically and functionally a unique structure of the central nervous system (CNS). The primary function of the chiasm is to allow registration of each visual hemifield on the contralateral visual cortex, thereby allowing binocular vision. The optic chiasm contains approximately 2.4 million nerve fibers as the two optic nerves join. Slightly more than half of the fibers (those from the nasal half of the retina) decussate and join the uncrossed temporal fibers of the contralateral optic nerve to form the optic tracts (Mikelberg et al., 1989). The chiasm can be compressed by several types of lesions given its unique location. Among the causes of chiasmal compression, pituitary adenomas are the most frequent benign tumors. In the parasellar region, meningiomas can compress both the chiasm and the optic nerves and invade the surrounding anatomical structures such as the cavernous sinus (Schiefer et al., 2004). Other significant compressive lesions are craniopharyngiomas and vascular abnormalities. Astrocytomas may infiltrate the chiasm. The pattern of visual dysfunction depends predominantly on the location of the lesion and the position of the chiasm. Chiasmal compression can result in visual dysfunction through several mechanisms including metabolic, ischemic and mechanical insults (Ito and Di Polo, 2017; Morgan, 2004; Piette and Sergott, 2006). Both retrograde and anterograde degeneration have been demonstrated in response to chiasmal compression (Kanamori et al., 2012). One unique aspect of chiasmal compression is that profound visual loss can often be dramatically reversed within hours following surgical decompression. In 1915, Cushing and Walker first reported visual recovery following pituitary tumor resection (Cushing and Walker, 1915). However, it has become clear over the past century that the visual outcome following decompression varies widely, ranging from permanent vision loss to complete visual recovery. The mechanisms by which retinal ganglion cell (RGC) axons can be injured and then recover have been investigated, and many pre-operative anatomical and functional factors have been explored as predictors of visual outcome. With recent advances in technology, we now have a diverse range of tools to evaluate the anatomical and functional integrity of the visual pathway before and after decompression therapy.

This review summarizes the pattern of vision loss and recovery in patients with chiasmal compression, and our current understanding of the mechanism of this reversible vision loss. We then review the latest advances in prognostic indicators of immediate and long-term post-decompression visual outcomes and their predictive strengths.

* Corresponding author.
E-mail address: helendm@gmail.com (H.V. Danesh-Meyer).
[1] % contribution made by each author in producing manuscript: Helen Danesh-Meyer 30%, Jinny Yoon 30%, Mitchell Lawlor 20%, Peter Savino 20%.

https://doi.org/10.1016/j.preteyeres.2019.06.001
Received 13 February 2019; Received in revised form 5 June 2019; Accepted 12 June 2019
Available online 14 June 2019
1350-9462/

Abbreviations

CNS	Central nervous system
RGC	Retinal ganglion cell
GCC	Ganglion cell complex
RNFL	Retinal nerve fiber layer
CSF	Cerebrospinal fluid
ipRGCs	Intrinsically photosensitive retinal ganglion cells
MRI	Magnetic resonance imaging
fMRI	Functional MRI
CT	Computed tomography
DTI	Diffusion tensor imaging
CE-FIESTA	Contrast material-enhanced fast imaging employing steady-state acquisition
VEP	Visual evoked potential
PERG	Pattern electroretinogram
PhNR	Photopic negative response
OCT	Optical coherence tomography

2. Vision loss in chiasm compression

2.1. Anatomy of the optic chiasm

The anatomical location of the chiasm renders it susceptible to compression damage from lesions arising from the surrounding structures. However, anatomic variations are common and influence the clinical presentation and type of visual field defects. The optic nerves rise from the optic canal to the chiasm at an angle of 15–45°. Below the chiasm lie the sella turcica, the pituitary gland, and the diaphragma sellae. While most commonly the chiasm lies over the diaphragm sellae (80%), it can occupy a 'pre-fixed' position when lying above the tuberculum sellae (in 15–20%) and 'post-fixed' when it lies above or behind the dorsum sellae (approximately 4%) (Griessenauer et al., 2014; Miller et al., 2005) (Fig. 1).

The basal cistern, a cerebrospinal fluid (CSF)-filled cavity, separates the chiasm from the diaphragm sellae. The chiasm lies postero-superiorly within the wall of the third ventricle and anteriorly with the CSF within the chiasmatic cistern. Superior to the chiasm is the hypothalamus, bounded by the lamina terminalis which itself forms the anterior wall of the third ventricle. The chiasm invaginates the ventricle, separating the optic recess above and the infundibular recess below. The internal carotid arteries are located laterally on both sides (Csillag, 2003; Kidd, 2014). The anterior cerebral and anterior communicating arteries lie above the intracranial optic nerves and chiasm.

The chiasmal blood supply can be grouped into dorsal and ventral vessels. The dorsal group consists of branches from the internal carotid artery, anterior cerebral artery and anterior communicating artery, and the ventral group consists of the posterior communicating artery and basilar artery. Chiasmal circulation is characterized by significant inter-individual variation and a rich collateral network (Bergland, 1969). Ischemic infarct of the chiasm is, therefore, rare.

The organization of RGC axons in the anterior visual pathway is complex. Within the retina, the RGC axons follow a particular pathway as they enter the optic disc (Miller et al., 2005) (Fig. 2). The axons from the nasal macula project directly to the disc, forming the papillomacular bundle. These nasal macula retinal fibers decussate at the chiasm. The axons from the temporal macula arch around the nasal macular axons, forming the superior and inferior parts of the papillomacular bundle.

The peripheral axons from the temporal retina arch around the papillomacular bundle and enter the disc at the superior and inferior poles. These fibers from the retina temporal to the fovea remain uncrossed in the lateral part of the chiasm and project directly to the ipsilateral optic tract. The empirical evidence informing the proportion of crossed versus uncrossed fibers is limited. One autopsy study of a single human chiasm found a ratio of 53:47 (Kupfer et al., 1967), while a further study of a single human chiasm found a ratio of 56:43 using an

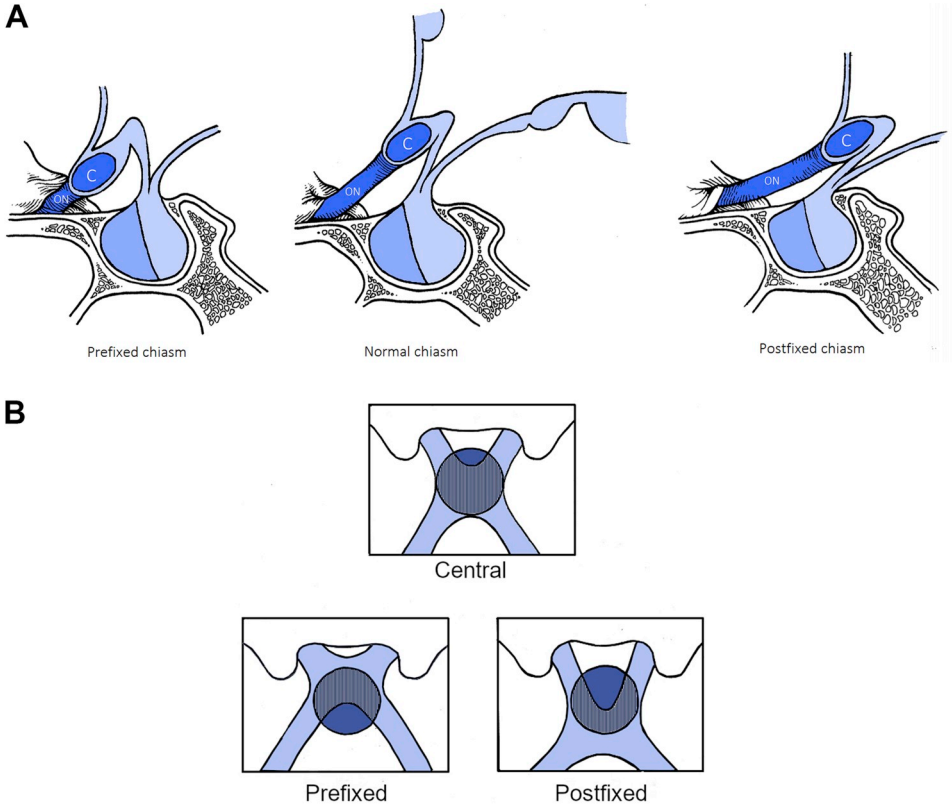

Fig. 1. a) Saggital view showing the relationship of the chiasm to the sella turcica. In the majority, the position of the normal chiasm is directly above the pitutary gland. In 15% the chiasm is 'prefixed', that is, it lies over the tuberculum sella. **b)** Schematic diagram demonstrating how the position the pituitary compresses different aspects of the chiasm.

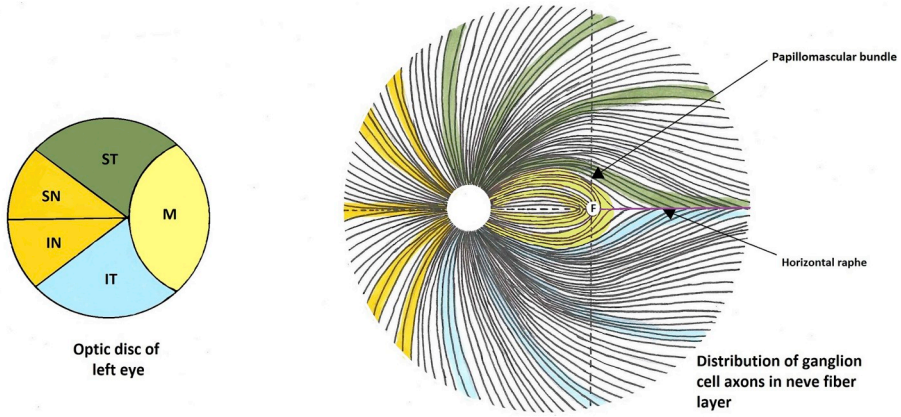

Fig. 2. Schematic represenstaion of the course of the retinal ganglion cell axons in the retin as they approach the optic nerve (left eye). The optic disc diagram shos the organisation of the axons in the optic nerve head. (M, medial; ST, superotemporal; SN, Superonasal;IN , inferonasal; IT, inferotemporal). The reitinal diagram demonstrates the course of the fibers from the retina to the optic nerve heard.

indirect assessment by looking at the ratio of crossed to uncrossed laminae in the lateral geniculate nucleus (Chacko, 1948).

However, more recent work has identified melanopsin-containing intrinsically photosensitive retinal ganglion cells (ipRGCs) as part of the input into the afferent arm of the pupillary light reflex (Hattar et al., 2003). It has also been shown that ipRGCs may show relative preservation in certain conditions such as mitochondrial optic neuropathies and normal tension glaucoma (Cui et al., 2015; La Morgia et al., 2010; Lawlor et al., 2017). It is unknown whether there is differential involvement of the ipRGCs with chiasmal compression.

The organization of axons in the optic nerve is comparable to that in the retina: axons from the papillomacular bundle run temporally within the anterior optic nerve, and then move centrally as the optic nerve moves posteriorly. Histological studies in primates and humans have demonstrated the central location of crossing fibers within the chiasm (Horton, 1997; Hoyt, 1970; Jeffery, 2001; Kupfer et al., 1967; O'Connell, 1973). The macular RGCs responsible for visual acuity and color vision lie centrally within the optic nerve and chiasm (Miller et al., 2005).

Within the chiasm, the crossing fibers from the superior retina cross in the caudal chiasm and enter the medial side of the optic tracts, whereas those from the inferior retina cross more rostrally entering the optic tract laterally (Hoyt and Luis, 1963). The uncrossed fibers from the inferior and superior retina maintain the retinotopic distribution within the lateral chiasm. Macular fibers make up a large proportion of the chiasm and contain both crossed and uncrossed fibers. Macular fibers are located superiorly and centrally, and are not present in the inferior regions of the chiasm (Hoyt, 1970). The optic tract, formed by the RGC axons from the ipsilateral temporal hemiretina and contralateral nasal hemiretina, continues towards the lateral geniculate nucleus.

The precise topographical arrangement of the crossing axons remains unclear. Ultra-high-resolution diffusion tensor imaging (DTI) of the post-mortem human chiasm identified the paracentral chiasm as the area with the most complex fiber architecture with considerable fiber curvature and crossing (Roebroeck et al., 2008). The paracentral areas show diagonal bands running from the antero-inferior aspect to the postero-superior aspect. The diagonal bands are thought to represent the nasal hemiretina fibers diverging from the ipsilateral optic nerve, and already crossed fibers merging into the contralateral optic tract. Similarly, an *in vivo* high-resolution DTI in healthy young subjects consistently identified a perimeter of low anisotropy in the paracentral chiasm, suggesting complex fiber orientation was occurring in this region (Sarlls and Pierpaoli, 2009). The current DTI-based technology, however, lacks spatial resolution to identify the individual orientation of crossed and uncrossed fibers within the chiasm (Hofer et al., 2010; Kamali et al., 2014; Staempfli et al., 2007). Silver-stained human post-mortem chiasm showed that the crossing fibers formed plaits in the central chiasm and that the central chiasm consisted of multiple plaits, each measuring around 50 μm-wide (Neveu et al., 2006). Jain et al. obtained high-resolution photomicrographs from a post-mortem chiasm sample sectioned at 5 μm intervals (Jain et al., 2015). The photomicrographs from all the sections were integrated to give the direction of crossed fibers. The analysis confirmed the findings of the DTI studies. Crossings were seen in the paracentral chiasm, and the crossing areas were distributed in an antero-inferior to postero-superior arrangement. The crossing fibers did not simply cross the chiasm in a diagonal path; they curved sharply in a transverse direction to cross the central chiasm, and then curved sharply again to align with contralateral uncrossed fibers before entering the optic tracts. Most crossings within the paracentral chiasm occurred at near perpendicular angles, but lower angle transverse crossings and lower angle antero-posterior crossings occurred in the medial and lateral aspects of the paracentral chiasm, respectively.

Wilbrand's knee was initially described as a loop of crossing fibers from the inferonasal retina, deviating into the pre-chiasmal part of the contralateral optic nerve before entering the optic chiasm (Roebroeck et al., 2008; Sarlls and Pierpaoli, 2009). Wilbrand first identified these fibers in silver-stained sections from a human chiasm where one eye had been enucleated a number of years before death (Wilbrand, 1926). Wilbrand's knee was accepted as an explanation for the anterior junctional syndrome (ipsilateral central visual field defect and a contralateral temporal hemianopia respecting the vertical meridian) (Karanjia and Jacobson, 1999); however, the existence of Wilbrand's knee has been challenged (Horton, 1997). Horton investigated the anatomy of Wilbrand's knee in ten rhesus monkeys, three squirrel monkeys, and three humans. Of the ten rhesus monkeys, eight were normal, and the other two were each euthanized six months and four years after unilateral enucleation. Wilbrand's knee was not identified in any of the eight normal animals; a possible ‘early’ knee was seen in the animal six months post unilateral enucleation, whereas a definite knee was evident in the animal euthanized four years post unilateral enucleation. This evidence suggested that Wilbrand's knee was not present in normal monkeys, but was induced over time in association with optic nerve atrophy occurring secondary to enucleation. To confirm these findings in another primate species, Horton also examined three normal squirrel monkeys and found no evidence of Wilbrand's knee. Finally, Horton analyzed post-mortem human optic chiasm specimens obtained from three patients who had monocular enucleation for intraocular tumors. As with the rhesus monkeys, the presence of Wilbrand's knee appeared related to the time elapsed since unilateral enucleation: it was not identified in a patient who lost one eye five months prior to death, but was seen in those who had enucleation two and 28 years prior. Horton suggests that the atrophy of the remaining optic nerve causes traction upon the fibers from the contralateral inferonasal retina, and that Wilbrand's knee is an artifact of monocular enucleation. More recently, high-resolution diffusion tensor imaging (DTI) techniques have shown that the paracentral optic nerve contains complex fiber

orientations (Roebroeck et al., 2008; Sarlls and Pierpaoli, 2009). However, using photomicrographic image analysis of nerve fiber orientations in the human optic chiasm, Jain et al. identified high-angle crossings as far forward as the optic nerve–chiasm junction in the inferior parts of the chiasm (Jain et al., 2015). This could offer an anatomical explanation of junctional scotoma even if Wilbrand's knee does not exist as it was initially described. The 'junctional' scotoma could then be explained by incomplete compression of the chiasm rather than Wilbrand's knee (Lee et al., 2006).

2.2. Vision loss as presenting complaint

Patient's subjective visual complaints are frequently non-specific. Patients with chiasmal compression are identified through several different initial presentations: incidental finding, visual loss, headache, and hormonal derangement. The most common presenting symptom in patients with chiasmal compression is visual disturbance. Headaches and symptoms of endocrine dysfunction can occur in isolation or with visual symptoms (Foroozan, 2003). Among patients undergoing surgical decompression, 38–72% reported visual dysfunction as the main presenting symptom (Carrim et al., 2007; Ebersold et al., 1986; Ogra et al., 2014). The majority of patients complain of blurred vision and decreased or dimming of peripheral vision at presentation although symptoms regarding peripheral vision loss tend to be vague (McDonald, 1982). The average duration of visual symptoms at diagnosis ranges from 6 to 24 months (Barzaghi et al., 2012; Findlay et al., 1983; Gnanalingham et al., 2005; Poon et al., 1995).

Ophthalmoplegia and consequent diplopia occur in 2–10% of patients (Cohen et al., 1985; Farooq, 2010; Poon et al., 1995; Sullivan et al., 1991). Diplopia can arise from ophthalmoplegia if lesions invade into the cavernous sinus and directly compress the oculomotor nerves. Less commonly, patients can experience hemifield slide. This is the perception of binocular diplopia from complete bitemporal hemianopia and loss of overlapping temporal visual field in a patient with latent heterophoria. The symptom is the result of duplication of the images that are seen by two different sectors in the cortex. The range of eye movement is full, but patients experience difficulty in reading because of doubling of words, loss of words or intermittent double vision. However, it is not uncommon for patients to be asymptomatic in the presence of dense visual field defects with neuroimaging-proven

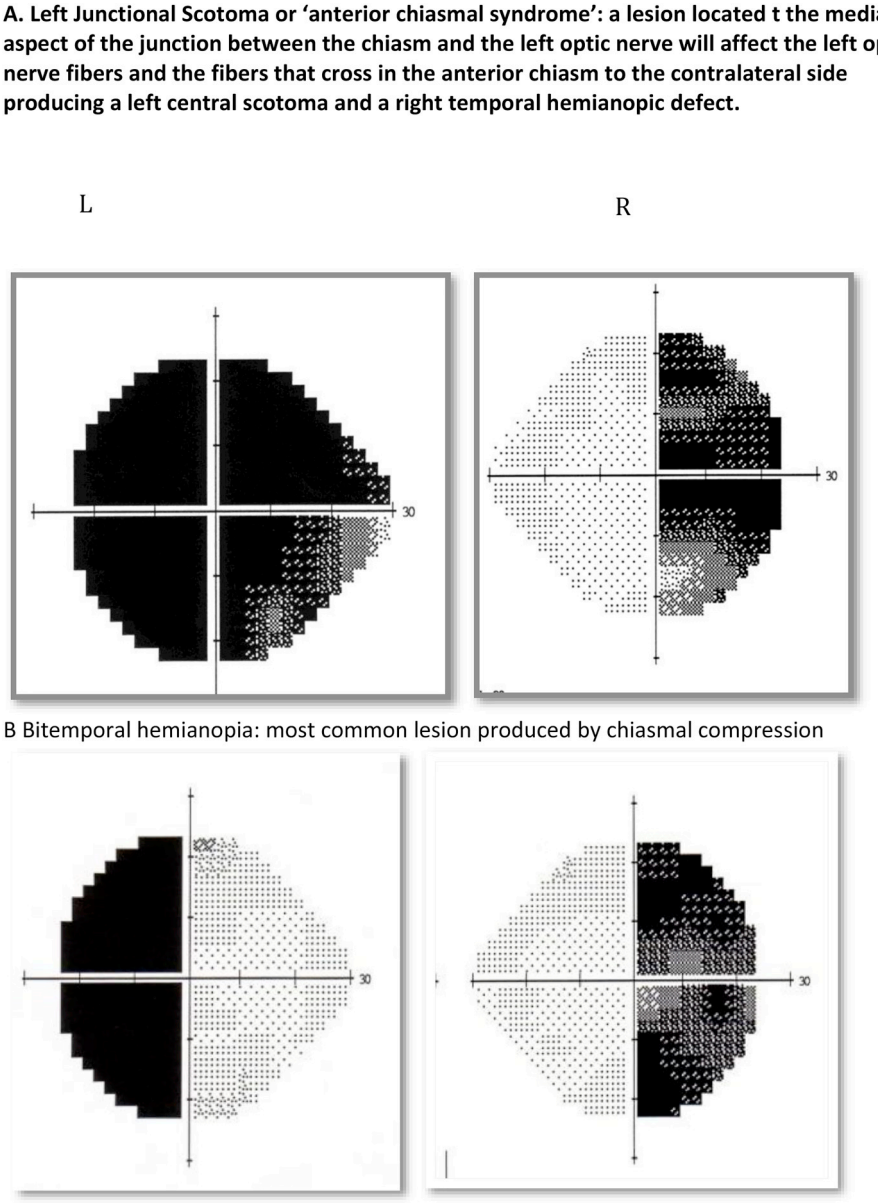

Fig. 3. Visual Field Defects Associated With Chiasmal Compression.

C. Unilateral hemianopia: a small lesion damaging only the crossing fibers of the right eye at the anteior chiasm can produce a monocular temporal hemianopic defect.

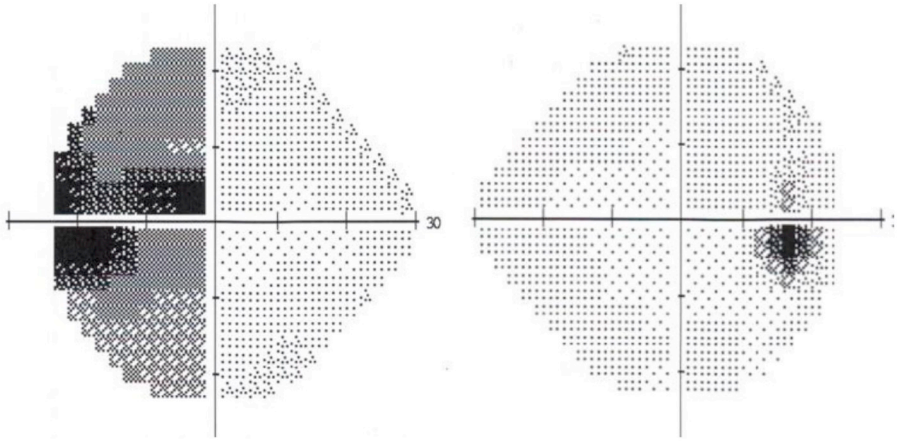

D. Right Incomplete incongruous hemianopia: pre-fixed chiasm or a tumor that impact on the optic tract

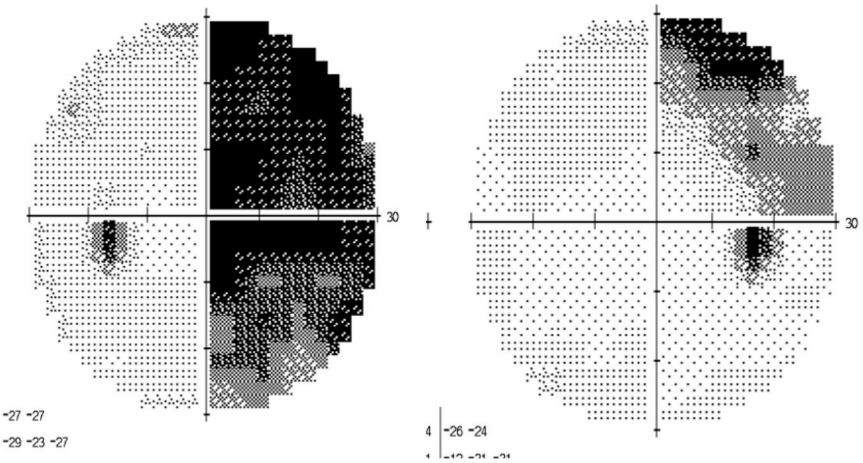

Fig. 3. (*continued*)

chiasmal compression (Cohen et al., 1985; Gnanalingham et al., 2005; Poon et al., 1995). Another uncommon feature of chiasmal compression is see-saw nystagmus which is a pendular oscillation that consists of elevation and intorsion of one eye and depression and extorsion of the contralateral eye. This suggests the loss of crossed visual input from the decussating fibres of the optic nerve at the level of the chiasm as the cause or lesions in the rostral midbrain.

2.3. Characteristics of vision loss in chiasmal compression

Compression of RGC axons at the chiasm usually first affects visual fields. Fig. 3 demonstrates the different patterns of visual field defects associated with chiasmal compression. The complexity of the decussation of fibers, inter-individual microanatomical diversity, individual variation in the relationship between the chiasm and skull base, the type and location of lesions, and the degree of compression all contribute to varying patterns of visual field defects. In addition, the results of studies depend on the selection and referral bias of the study population. Pituitary macroadenomas may compress the chiasm if they grow more than 8 mm above the diaphragm sella as smaller lesions do not come in contact with the chiasm.

Bitemporal hemianopia respecting the vertical meridian is a pathognomonic sign of chiasmal compression because compression preferentially damages the crossed fibers from the nasal hemiretina. It is also the most common type of visual field defect at diagnosis in most studies, occurring in 32–81% of patients with visual impairment (Barzaghi et al., 2012; Cohen et al., 1985; Goyal et al., 2013; Klauber et al., 1978; Ogra et al., 2014; Peter and De Tribolet, 1995; Poon et al., 1995; Rivoal et al., 2000; Schmalisch et al., 2012; Sullivan et al., 1991; Trobe et al., 1984) (Table 1). In our prospective study of 103 patients with chiasmal compression, 41% had bitemporal hemianopia (either complete or incomplete) (Ogra et al., 2014). Of these patients, the mean visual acuity was 6/7.5 suggesting that central acuity is often preserved despite significant visual field deficits. Half of our patients with bitemporal defects had asymmetric visual field abnormalities. Asymmetric deficits are common as the lesion does not necessarily exert the same effect on all fibers. Patients with unilateral or asymmetric bilateral visual field loss demonstrate a relative afferent pupillary defect, which is present in 15–77% of the patients prior to chiasmal decompression (Poon et al., 1995; Trobe et al., 1984). Infrasellar lesions initially produce superotemporal visual field defects, which progress in a clockwise direction in the right eye and in an anticlockwise direction in

Table 1
Literature review of studies that report distribution of patterns of visual field defects in patients with pituitary neoplasms.

Year	1968	1968	1973	1981	1984	1985	1990	1991	2000	2004	2012	2014
Author	Wilson et al. (9)	Elkington et al. (10)	Hollenhorstet al.(11)	Fahlbusch et al. (12)	Trobe et al.(13)	Cohen et al.(14)	Mohr et al. (15)	Comtois et al.(16)	Rivoal et al. (17)	Schiefer et al.(6)	Schmalish et al. (18)	Ogra et al.
N (Pts)	50	260	1000	285	49	100	74	93	307	153	69	101
Visual Acuity	Not reported	Not reported	Not reported	Not reported	6/6-6/12 = 37% > 6/15 = 63%	6/6-6/9 = 47% > 6/12 = 53%	Not reported	Visual acuity reduction in 54%	Not reported	Not reported	Not reported	*
Visual field testing	NS	NS	NS	NS	NS	Kinetic	NS	Goldman	Goldman	Tuebingen**	SAP or Goldman	SAP
Type of VFD (%)												
Bitemporal Hemianopia	36*	71	30	48	45	54	53	54	32	1	81.2	41
Bitemporal quadrantanopia			10	5		17	10	15	15	20		
Homonymous defect	6	5	4	2	4	1	1		3	11	1.5	13
Junctional syndrome	6	7.3	17	11	39	15	10		5	13	7.2	4
Central Scotoma		0.4	30			4				19		5
Unilateral defect	4	9	6	13	8	7	8	26	32	13	10.1	33

the left eye as the tumor grows (Barzaghi et al., 2012; Poon et al., 1995). Suprasellar lesions, on the other hand, affect inferotemporal quadrants first (Chen et al., 2003). Meningiomas can affect any part of the anterior visual pathway, including tuberculum sellae, sphenoid ridge, olfactory groove, anterior clinoid process, spheno-orbital or frontal base, and hence cause a wide range of visual field defects (Park et al., 2015; Sleep et al., 2003). Junctional scotoma, occurring when the pre-chiasmal area is compressed, is a common pattern of visual field defect seen in 4–39% of patients presenting for decompression surgery (Cohen et al., 1985; Ogra et al., 2014; Schiefer et al., 2004; Trobe et al., 1984). Other types of visual field defects seen in chiasmal compression include unilateral defects and homonymous hemianopias. Unilateral defects can occur when the compression is at the cranial portion of the optic nerve. Homonymous hemianopias can occur if the chiasm is prefixed; if only the lateral chiasm is involved; or if the lesion is predominantly compressing the optic tract (Glisson, 2014; Ogra et al., 2014). Bilateral temporal hemianopic scotomas can occur if only macular fibers are involved.

Visual acuity is variably affected in chiasmal compression, ranging from normal to no light perception (Barzaghi et al., 2012; Cohen et al., 1985; Gnanalingham et al., 2005; Klauber et al., 1978; Ogra et al., 2014; Poon et al., 1995; Rivoal et al., 2000; Schmalisch et al., 2012; Sullivan et al., 1991; Trobe et al., 1984). Color vision deficits may be present if visual acuity is decreased; however, color vision deficits are often present when visual acuity is preserved but visual field deficits are present (Barzaghi et al., 2012; Danesh-Meyer et al., 2006a; Sullivan et al., 1991). The pre-operative mean best-corrected visual acuities were between 6/6 and 6/18 in different studies (Astorga-Carballo et al., 2017; Barzaghi et al., 2012; Danesh-Meyer et al., 2006a, 2008, 2015; Gnanalingham et al., 2005; Ogra et al., 2014). In our study, 40% of patients had visual acuity of 6/6 while 55% had vision 6/7.5 or better, with almost two-thirds achieving better than 6/9. Findlay et al. found that severe reduction in visual acuity was not seen until the field loss was more than 50% (Findlay et al., 1983). Other studies, in particular the more recent studies, have similarly reported good central visual acuity as diagnosis of lesions are likely occurring at earlier stages due to improved neuroimaging (Klauber et al., 1978; Peter and De Tribolet, 1995; Sullivan et al., 1991; Yoneoka et al., 2015).

The reason why the crossing fibers are vulnerable to chiasmal compression is still under debate. The mechanical theory is supported by direct observation of selective injury to the crossed fibers in *ex vivo* chiasmal compression models (Hedges, 1969; Kosmorsky et al., 2008). In these models, an expanding balloon tip of a Foley catheter was inserted into the empty sella in fresh, human autopsy brain tissue to simulate a rapidly expanding chiasmal mass lesion. The expansion of the balloon led to the elevation of the chiasm and stretching of mostly the nasal crossed axons (Hedges, 1969). The pressure in the central chiasm was consistently higher than the pressure in the lateral chiasm during balloon expansion, indicating that the crossed fibers are inherently more prone to a deformation stress (Kosmorsky et al., 2008).

McIlwaine et al. proposed a simple mechanical hypothesis to explain preferential damage to the crossing fibers (McIlwaine et al., 2005). Unlike the noncrossing temporal fibers, the crossing fibers are in contact with each other at the point of decussation. The area of contact is subject to greater pressure at any given external compressive forces, since pressure is inversely proportional to the area over which the force is applied. This hypothesis has been tested using a computerized model of chiasmal compression (Wang et al., 2014a, 2014b, 2016). A multiscale analysis showed that the strain distribution in the crossed fibers was much more non-uniform and higher than in the uncrossed fibers, and the strain distribution progressed upwards with increasing pressure from beneath. The authors found the crossing angle was the most significant parameter that affected the strain (Wang et al., 2016). The findings from the simulated model match the data obtained from the *ex vivo* human chiasm. In the post-mortem chiasm specimen, the crossing fibers were found almost perpendicular to each other, supporting the

selective vulnerability of these fibers (Jain et al., 2015). The estimated pressures within the simulated chiasm were comparable to the pressures measured in the *ex vivo* chiasmal compression model (Kosmorsky et al., 2008). The simulated model explains why chiasmal compression initially causes bitemporal hemianopia, but the model requires further clinical validation. It is possible that both vascular and mechanical insults have a role in bitemporal hemianopia.

The vascular theory is based on the observation from a detailed autopsy study by Bergland (1969). The chiasm receives blood supply from dorsal and ventral groups of blood vessels, but the central part of the chiasm only receives blood supply from the ventral vessels (Bergland, 1969). An infrasellar lesion may disturb the ventral blood vessels, thereby selectively affecting the central crossed fibers. Their hypothesis, however, requires an assumption that no anastomoses exist between the dorsal and ventral circulations and does not explain bitemporal hemianopia caused by suprasellar lesions. An autopsy study identified the central chiasm as the weak point of microcirculation due to sparse capillary distribution, and a shared blood supply between the inferior part of the chiasm and the pituitary gland (Lao et al., 1994). The authors speculate that even in the absence of compression, ischemia of the central chiasm may occur due to the pituitary tumor "stealing blood" through the shared blood supply. This hypothesis is yet to be validated and in our experience is unlikely to have clinical relevance.

2.4. Risk factors for pre-operative visual dysfunction

2.4.1. Size of tumor

Studies have evaluated the relationship between the degree of suprasellar extension on neuroimaging and impairment in visual acuity (Ho et al., 2015; Schmalisch et al., 2012; Wang et al., 2008) and visual field (Findlay et al., 1983; Ho et al., 2015; Ikeda and Yoshimoto, 1995; Monteiro et al., 2010b; Schmalisch et al., 2012; Wang et al., 2008). In these studies, the degree of suprasellar extension was measured on magnetic resonance imaging (MRI) as the distance between the position of the chiasm and a reference line joining the frontal base and posterior clinoid process on sagittal views, or a reference line between the upper surfaces of the internal carotid arteries on coronal views. Suprasellar extension between 8 and 15 mm above the sagittal reference line was associated with visual impairment (Ikeda and Yoshimoto, 1995; Schmalisch et al., 2012), with the greater the extension the more severe the visual impairment. However, while this was a general trend, it was not a consistent finding. Cross-sectional area of the chiasm has also been studied and shown not to be a good predictor of visual field defect, presumably because the chiasm can spread horizontally when compressed and the cross-sectional area will remain unchanged (Carrim et al., 2007).

Tumor volume showed less correlation with visual disturbance. Whole tumor volume was poorly correlated with temporal visual field loss (Hudson et al., 1991). The diameter of the pituitary adenoma was weakly correlated with visual field defects (Kasputyte et al., 2013). Others showed a close correlation between the tumor diameter and the

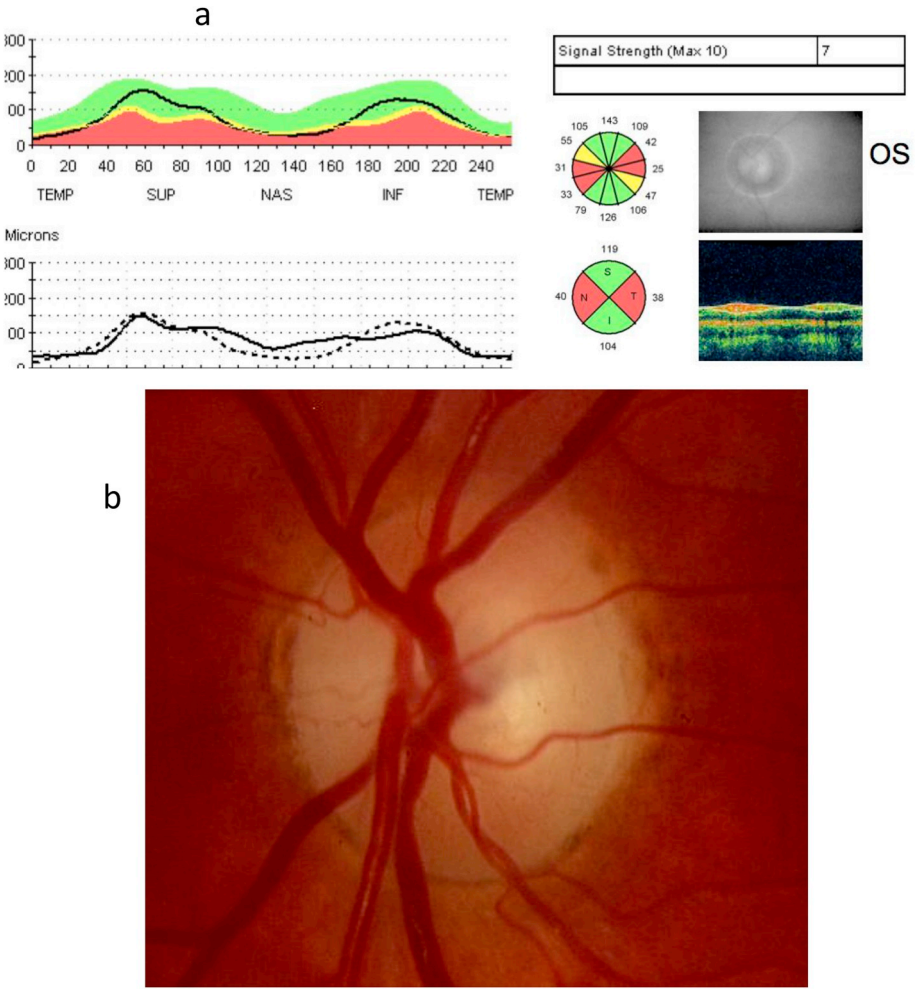

Fig. 4. a) Optical coherence tomography scan of a left optic nerve in a patient who had band atrophy from chiasmal compression. Note the preferential loss of retinal nerve fiber layer nasally and temporally. **b)** Optic nerve photo of the same patient.

visual field defect (Rivoal et al., 2000), between the tumor volume and pattern standard deviation (Lee et al., 2011), and between the cranio-caudal diameter greater than 30 mm and mean deviation (Barzaghi et al., 2012). The cranio-caudal diameter of the tumor was not correlated with color vision defects or decreased visual acuity (Barzaghi et al., 2012). The size or volume of a tumor does not consistently predict the extent of visual impairment because the tumor may grow laterally or downward, without affecting the chiasm. The direction of growth and site of compression may be more important in determining visual impairment. Two investigators showed that the position of the chiasm in relation to the pituitary tumor was important in determining visual impairment (Eda et al., 2002; Schmalisch et al., 2012). A correlation between visual field defect and the height of tumor only existed if the chiasm was located superior to the pituitary tumor. No such relationship was observed if the chiasm was anterior to the tumor. Prieto et al. also demonstrated that the direction of the force of compression and the pattern of distortion of the chiasm were important determinants of the degree of impaired visual acuity (Prieto et al., 2015). In general, it appears that the degree of visual impairment depends on how severely the chiasm is compressed although it is recognized that exceptions to this trend are not uncommon.

2.4.2. Duration of symptoms

The duration of symptoms at presentation has been inconsistently correlated with pre-operative vision loss. Several studies found a correlation between the duration of visual symptoms and visual field defects (Findlay et al., 1983; Gnanalingham et al., 2005). Duration of symptoms greater than 12 months was associated with a worse mean deviation, poorer visual acuity, more frequent reduction in color vision and optic disc pallor (Barzaghi et al., 2012). Duration of six months or longer was weakly correlated with visual acuity (Trobe et al., 1984). On the other hand, other researchers reported no correlation between the duration of symptoms and the degree of visual impairment (Goyal et al., 2013; Sleep et al., 2003; Wang et al., 2008). In our experience, there is a poor correlation between duration of symptoms and level of pre-operative vision loss.

Pituitary apoplexy can cause substantial visual impairment, even though the duration of symptoms may be as short as 24 h. Pituitary apoplexy occurs in 1.6–21% of pituitary tumors (Moller-Goede et al., 2011; Sanno et al., 2003), and is the result of spontaneous and large infarction of pituitary tumors. Secondary hemorrhage and edema lead to acute compression of surrounding structures, which in turn causes rapid deterioration in visual field defects, ocular motor nerve palsies or severe headaches (Randeva et al., 1999; Reid et al., 1985). Visual field defects, reduced visual acuity and ocular motor palsies are observed in up to 80% of patients with apoplexy (Ayuk et al., 2004; Moller-Goede et al., 2011; Mou et al., 2009).

2.4.3. Optic atrophy

Chronic compression of the chiasm may lead to degeneration of RGCs and its axons, or optic atrophy. With chronic compression, RGCs originating from the retina nasal to the fovea are preferentially lost. These include the fibers from the nasal macular RGCs which course directly to the temporal disc, and axons from the peripheral RGCs coursing into the nasal part of the disc. Hence, damage to these fibers by compression at the chiasm leads to 'bow-tie' or 'band atrophy' (as these fibers are located in the nasal and temporal sectors of the optic disc). As the temporal retinal ganglion fibers do not decussate into the chiasm, they are relatively spared by chiasmal compression, accounting for the relative preservation of the fibers of the superior and inferior optic disc (Fig. 4).

There are two available histopathologic examinations of the optic nerve in patients with optic atrophy secondary to chiasmal compression. Unsold and Hoyt showed that the arrangement of fibers destined to cross in the chiasm begins anterior to the optic canal in the intraorbital optic nerve (Unsold and Hoyt, 1980). Mikelberg demonstrated profound preferential loss of the nasal fibers but only approximately 50% loss of superior and inferior fibers. There was variable loss of the temporal fibers in the temporal sectors, presumably due to the distribution of the crossing fibers (Mikelberg and Yidegiligne, 1993).

Our work quantified the distribution of retinal nerve fiber layer (RNFL) loss at the optic nerve head when the site of damage is at the chiasm. We quantified optic atrophy in patients with chiasmal compression using OCT peri-papillary RNFL measurements (Danesh-Meyer et al., 2006a). Our data demonstrated that loss of RNFL correlated with the severity of visual field loss as measured by automated perimetry. Furthermore, there was diffuse loss in all sectors even in patients with strict bitemporal hemianopic defects with loss ranging from 20 to 35% (Danesh-Meyer et al., 2006a). However, the temporal and nasal sectors showed proportionally greater thinning which is consistent with the clinical appearance of 'band atrophy' with loss ranging from 40 to 65%. Three smaller studies using OCT and scanning laser polarimetry in chiasmal compression, have also demonstrated diffuse thinning of the RNFL in addition to preferential thinning of the temporal and nasal sectors (Kanamori et al., 2004; Monteiro et al., 2003, 2004).

The clinical diagnosis of optic atrophy is based on pallor of the optic disc, narrowing of the retinal vasculature, and loss of RNFL reflexes. Early nerve fiber loss manifests as wedge defects, or dull and dark red streaks in the supero- and inferotemporal arcuate nerve fiber layers (Lundstrom and Frisen, 1976; Newman et al., 1982). In approximately 10% of cases, non-glaucomatous 'cupping' or excavation of the disc has been documented to occur (Unsold and Hoyt, 1980). The evaluation of optic disc color is subjective and variable as the clinical interpretation of pallor does not necessarily correlate with the amount of measured nerve fiber layer loss or the level of visual function. The reported incidence of optic atrophy in patients undergoing chiasmal decompression varied widely from 16 to 71% (Carrim et al., 2007; Cohen et al., 1985; Gnanalingham et al., 2005; Klauber et al., 1978; Poon et al., 1995; Powell, 1995; Schmalisch et al., 2012; Sullivan et al., 1991; Trobe et al., 1984), likely representing differences in patient cohort characteristics, but also inconsistency in clinical grading of optic atrophy. Disc appearances are graded using descriptive terms, such as slight, diffuse or severe (Cohen et al., 1985; Klauber et al., 1978), or partial or total (Lundstrom and Frisen, 1977). Grading of optic nerve pallor is known to have high inter-observer variability and can be influenced by media opacity, refractive error, individual anatomic variation and pseudophakia (Abrams et al., 1994; Spry et al., 1999). In general, optic atrophy is more likely to be associated with abnormal pre-operative visual field, visual acuity and color vision (Lundstrom and Frisen, 1976; Poon et al., 1995; Schmalisch et al., 2012; Trobe et al., 1984), but clinical grades of optic atrophy are poorly correlated with the degree of visual field defect (Lundstrom and Frisen, 1977).

Several investigators have evaluated methods for improving the grading of optic pallor including enlarged high-contrast black and white prints (Berkowitz and Balter, 1970; Schwartz et al., 1973), estimating optic atrophy by color contrast, and quantifying the degree of atrophy by microdensity in the blue (470 nm) and in the red (640 nm) regions (Davies, 1970; Sorensen, 1979). However, these techniques require methods unavailable in standard clinical practice and demand a high degree of familiarity with the techniques.

3. Proposed mechanism of vision loss

Mechanisms of visual loss with long-standing compression of the chiasm or optic nerve have not been completely characterized. The original work by Clifford-Jones in a feline optic nerve compression model in the 1980s suggests that the changes include overlapping processes of demyelination, glial proliferation, remyelination and Wallerian degeneration (Clifford-Jones et al., 1980, 1985). Other investigators have reported that conduction block and axoplasmic stasis occur in the early stages. Finally, although the optic nerve is CNS and

not peripheral nerve, the existing large body of work on peripheral nerve compression may assist in providing further insights into the mechanism of vision loss. The most notable feature of vision loss with chiasmal compression is that decompression can result in immediate improvement in visual function (within minutes to hours). Such rapid recovery does not occur with other forms of optic nerve injury.

3.1. Conduction block

Compression of a nerve produces a conduction block where an action potential fails to propagate past the compression point. Specific electrophysiological abnormalities in chiasmal compression are described in detail in section 5.5. Here, we review the underlying mechanism by which conduction block may impair optic nerve and chiasmal function. Several different processes are thought to be involved in reversible conduction block including mechanical deformation of nerve fibers, focal ischemia at the point of compression, changes in ionic gradient across the axonal membranes and demyelination (Halliday et al., 1976; Janaky and Benedek, 1992). Ionic gradient alterations include accumulation of potassium ions and entry of calcium into the axoplasm. There is also suggestion of disruption to the axon cytoskeleton (Cottee et al., 2003).

Conduction block can be observed within minutes of nerve compression. In experimental baboon and rodent studies, pneumatic cuff compression of peroneal nerves achieved rapid conduction block that was accompanied by mechanical displacement of the Nodes of Ranvier, decreased fascicular area, compression of axoplasm, and stretching of internodes (Dyck et al., 1990; Ochs and Hollingsworth, 1971). Regulation of node assembly and internode distance are crucial for effective transmission of the action potentials and disruption of nodal architecture has been shown to slow down conduction markedly (Funch and Faber, 1984; Seidl, 2014).

Nerve compression can also cause reversible conduction block via disruption of the cytoskeleton (Cottee et al., 2003). In animal optic nerve crush models, loss of neurofilament immunoreactivity and failure of both anterograde and retrograde axonal transport of a fluorescent dye have been demonstrated (Hanke and Sabel, 2002; Maxwell et al., 1997). Pressure on nerves stretches the axonal plasma membrane, leading to uncontrolled entry of calcium and the disruption of microtubules (Maxwell et al., 1997). Disturbance to the retrograde supply of neurotrophic factors from the superior colliculus has been shown to lead to rapid reduction of pattern electroretinogram (PERG) amplitudes in rat models (Chou et al., 2013). Reversible changes in visually evoked potentials (VEPs) with acute compression of the intraorbital optic nerve have suggested a role with alterations in axonal conduction and transient disruption of vascular supply (Janaky and Benedek, 1992). The reversibility of conduction block is further discussed in Section 4.2.

3.2. Ischemic injury

Ischemic injury is considered to play a role both in acute compression as well as long-term compression. Peripheral nerve compression has been shown to lead to disruption of perineural microcirculation (Gao et al., 2013). In conditions where compression is position-dependent and nerve dysfunction is intermittent, such as in carpal tunnel syndrome, leg crossing peroneal nerve palsy, and tourniquet paralysis, the altered nerve excitability properties are very similar to those induced by ischemia, indicating focal ischemia as an underlying mechanism for reversible conduction block (Campbell, 2008; Ikemoto et al., 2009; Kuwabara, 2009; Yates et al., 1981). Anoxic condition and blockage of oxidative metabolism have been closely associated with rapidly reversible conduction block in animal peripheral nerves (Ochs and Hollingsworth, 1971). It is thought that metabolic products of focal ischemia interfere with the recovery of sodium channels without structural damage, resulting in rapidly reversible conduction block (Grosskreutz et al., 2000).

In terms of chiasmal compression, Hoyt postulated in 1970 that collapse of the capillaries is unavoidable under compressive forces great enough to distort and stretch the chiasm (Hoyt, 1970). Evidence for a role for ischemia in compression can be extrapolated from cases of gaze-evoked amaurosis. In gaze-evoked amaurosis, there is transient decrease of vision as a result of compression of the optic nerve in the orbit against a space-occupying lesion (such as tumor or foreign body) with eccentric gaze. Vision is restored when gaze is returned to the primary position. Evidence suggests that the loss of vision with eccentricity is predominantly due to disruption of the optic nerve microvasculature or compression of the central retinal artery compromising circulation (Otto et al., 2003). Furthermore, gaze-evoked amaurosis was shown to result in complete disappearance of the arterial waveform in the central retinal artery with Doppler ultrasound imaging (Knapp et al., 1992). Decrease in perfusion to the optic nerve head and surrounding choroidal and retinal arterioles has also been demonstrated with fluorescein angiography (Jakobiec et al., 1984). We have reported a patient who demonstrated a complete loss of the VEP waveform on eccentric gaze (without any corresponding changes in retinal vasculature on clinical examination) which returned to normal in the primary position (Danesh-Meyer et al., 2001). This finding suggests that the underlying mechanism may also include a component of disruption of axonal conduction.

(Lange et al., 1994).

3.3. Demyelination

Demyelination results in impaired function because the demyelinated axon membrane lacks an adequate regenerative ionic mechanism to efficiently transmit action potentials (Cottee et al., 2003; Kiernan and Kaji, 2013; Ritchie and Rogart, 1977). Demyelination also has been shown to expose voltage-gated potassium channels at the juxta-paranodal sites in *ex vivo* and *in vivo* spinal cord crush injury models (Ouyang et al., 2010). In these models, activation of the potassium channels inhibited action potential propagation, and the pharmacological potassium channel blockade led to enhanced conduction. Demyelinated axons eventually develop sodium channels, allowing low-velocity conduction (Bostock and Sears, 1978).

In the seminal studies by Clifford-Jones et al. in an *in vivo* feline chronic optic nerve compression model, histological loss of myelin was observed after two days of inserting a silicone balloon into the orbit (Clifford-Jones et al., 1980). Within one week, extensive demyelination took place, along with anterograde (or Wallerian) degeneration and astrocytosis. At five weeks, remyelination of the fibers was observed despite the presence of the compression balloon. Both remyelinated fibers and partially demyelinated fibers co-existed, although the new myelin sheaths were abnormally thin and short (Clifford-Jones et al., 1985).

In osteopetrotic mutant mice where stenosis of the optic canal chronically compresses the optic nerve, decreased local blood volume was demonstrated at the compression site, and this was correlated with loss of glial cells, increased apoptotic marker expression, and localized demyelination at postnatal day 30 (Kondo et al., 2013). At seven months, there was partial recovery of nerve cross-sectional area and the number of myelinated axons. This study also suggests that demyelination is part of the pathophysiology of optic nerve compression. Studies of peripheral nerve compression injury suggest that both ischemic damage and mechanical shear stress contribute to demyelination secondary to compression (Menorca et al., 2013).

In humans, anterograde demyelination of the optic tracts has been demonstrated using DTI. DTI allows for the non-invasive quantification of the restricted random motion (Brownian motion) of water molecules in the human brain. The degree of directionality of diffusion, often expressed as fractional anisotropy, depends primarily on the parallel organization of the axonal membranes, which restricts diffusion. Demyelination increases the radial diffusivity (diffusion perpendicular

to the axons), and does not affect axial diffusivity (diffusion parallel to the axons) (Song et al., 2003, 2005). Axonal degeneration, on the other hand, decreases axial diffusivity and does not affect radial diffusivity. An increase in radial diffusivity and/or a decrease in axial diffusivity will result in a decrease in fractional anisotropy (Lilja et al., 2017). Patients with pituitary adenomas had increased radial diffusivity and axial diffusivity in the optic tracts, while healthy controls and those with non-compressive tumors had normal radial diffusivity (Paul et al., 2014).

3.4. Retrograde degeneration

Retrograde degeneration begins at the site of the injury and then spreads towards the cell body. With chiasmal compression the cell body lies in the retina. Numerous models of RGC axonal damage (such as optic nerve crush, or elevation in intraocular pressure) have clearly demonstrated retrograde degeneration. These injuries can trigger a series of events locally, including accumulation of intracellular calcium ions, destabilization of the transmembrane potential, depolymerization of microtubules, activation of calcium-dependent proteases, pro-apoptotic enzymes, self-destruct programme, and eventually local axonal dissolution (Berkelaar et al., 1994; George et al., 1995; Ghaffarieh and Levin, 2012; Knoferle et al., 2010; Raff et al., 2002). An important cellular process disrupted by localized axon injury is axonal transport of neurotrophic support to RGCs, which has been shown to activate apoptotic pathways (Almasieh et al., 2012; Takihara et al., 2011). Once apoptotic pathways have been activated, retrograde degeneration follows.

There are a few studies that have investigated retrograde degeneration with compressive lesion of the optic nerve or injury to the tract or chiasm. Feline optic nerve electrolytic lesion (where direct electric current was delivered to the optic tract midway between the optic chiasm and the lateral geniculate nucleus) and axotomy both caused retrograde degeneration (Lin and Ingram, 1974a, 1974b). In osteopetrotic mutant mice, where the optic nerve is chronically compressed by stenosed optic canal, increased apoptosis was detected in the ganglion cell and inner nuclear layers, indicating retrograde spread of axon injury (Kawamura et al., 2010).

A few researchers used *in vivo* imaging techniques to demonstrate retrograde degeneration in real time. DTI in a mouse optic nerve crush model showed decreased axial diffusivity (indicating axonal degeneration) at proximal sites 300–600 μm away from the crush injury as early as 6 h post injury (Zhang et al., 2011). In humans, long-standing chiasmal compression causes preferential retrograde degeneration of crossing fibers although there is generalized loss of RGC as well. The preferential retrograde degeneration manifests as band atrophy and permanent visual field defects. Traditionally, the degree of RGC axon loss could only be estimated by subjective grading of disc atrophy or histological examination of post-mortem brain tissue (section 2.4.3. Optic atrophy). The structural loss can now be objectively quantified *in vivo* by optical coherence tomography (OCT) of the RNFL and macula. The specific patterns of RNFL and GCC defects are discussed in detail in section 5.6.

Two studies suggest optic nerve MRI signal abnormalities as evidence of retrograde degeneration. Tokumaru et al. showed T2-signal hyperintensity in the optic nerves at the site of compression in approximately half of patients with pituitary macroadenoma (Tokumaru et al., 2006). The presence of signal intensity was associated with the degree of compression, decreased pre-operative visual acuity, and reduced likelihood of post-operative visual acuity improvement. Watanabe et al., using highly sensitive MRI contrast material-enhanced fast imaging employing a steady-state acquisition (CE-FIESTA) technique, showed signal hyperintensities along the optic nerve (Watanabe et al., 2012). CE-FIESTA MRI can show fine anatomic details by increasing the relative contrast between the cranial nerves and the tumor. The CE-FIESTA hyperintense signals predicted persistent post-operative visual impairment with a sensitivity of 75% and a specificity of 96%. The authors suggest that the CE-FIESTA signal abnormalities represent retrograde irreversible cell damage. The identity of the MRI signal abnormalities needs further characterization in future studies.

The process of retrograde degeneration appears to be linked with demyelination. Paranodal demyelination and axonal degeneration have been shown to occur simultaneously during compression (Dyck et al., 1990).

3.5. Anterograde degeneration

Chiasmal compression may cause direct anterograde degeneration (or Wallerian degeneration) of the optic tract. Lilja et al. investigated changes in the optic tract with DTI in patients with chiasmal compression and visual field deficits (and controls) prior to surgical chiasmal decompression (Lilja et al., 2017). They found excellent correlation between radial diffusivity and visual field defects suggesting an anterograde demyelination in the optic tract caused by an increased tumor effect. The low level of axial diffusivity may represent early axonal degeneration in the optic tract (Lilja et al., 2017).

Transsynaptic anterograde degeneration will also lead to changes in the lateral geniculate nucleus, optic radiations, and neurons in the visual cortex. We explored the correlation between retinal nerve fiber thickness as measured by OCT and changes in the optic radiation and visual cortex in 17 patients with chiasmal compression, 10 who had no post-decompression visual field deficits and 7 with persistent visual field abnormality and RNFL thinning (Phal et al., 2016). Anterograde degeneration in the optic radiation was assessed using DTI and functional MRI (fMRI). We assessed mean radial diffusivity, axial diffusivity, mean diffusivity, and fractional anisotropy as well as fMRI BOLD signal. We found that surgically irreversible visual field defects were significantly associated with lower fractional anisotropy and higher diffusivities in optic radiations and lower visual cortical activation on fMRI. These changes suggest that both ischemic and demyelinating changes occurring within the optic radiations and visual cortex in patients who have permanent deficits with chiasmal compression. These findings suggest transsynaptic changes occur in the optic radiations and visual cortex.

3.6. Other proposed mechanisms

Other possible theories have been proposed although they remain speculative. One such theory is that local vasoconstrictor substances could potentially play some role in chiasmal ischemia with chronic compression. Pituitary tumors may cause local ischemia by elevating levels of endothelin-1. Endothelin-1 is only detected in pituitary tumors, and not in normal pituitary glands (Lange et al., 1994). It is a potent vasoconstrictor which has been shown to cause focal ischemia and RGC loss, leading to glaucoma-like optic neuropathies in animal models (Cioffi, 2005; Salvatore and Vingolo, 2010). The role in chiasmal compression, however, remains unsubstantiated. Frank ischemia of the chiasm from compressive lesions is rare owing to the rich collateral circulation and slow-growing nature of most perichiasmal lesions.

Another theory suggest that blockage of CSF circulation could have a role. Pre-operative MRIs of patients with perichiasmal tumors including craniopharyngioma, pituitary tumor, germ cell tumor and lymphoma have shown edema-like T2 signal hyperintensities along the optic tracts (Hirunpat et al., 2005; Nagahata et al., 1998; Saeki et al., 2003). The edema-like signal was localized to the middle portion of the optic tract where a large Virchow-Robin space is normally seen (Saeki et al., 2003). Virchow-Robin spaces are the CSF-filled perivascular outlet channels which drain interstitial fluid into the subarachnoid space. In the post-operative MRIs the edema-like signals disappeared or decreased, and the Virchow-Robin spaces reappeared (Nagahata et al., 1998; Saeki et al., 2003). The edema-like signals seem to be more

common in craniopharyngiomas, probably because they are frequently located behind the chiasm near the outlets (Nagahata et al., 1998).

Whether the edema-like signals and dilated Virchow-Robin spaces have a role in the pathogenesis of vision loss remains unanswered. The edema-like signals were not correlated with tumor size or degree of visual impairment (Nagahata et al., 1998; Saeki et al., 2003). However, the appearance of this radiological sign coincided with the development of visual symptoms in two patients with pituitary metastases (Saeki et al., 2001). The relationship between the blockage of CSF and vision loss requires further characterization and it remains unclear whether this plays a role in visual loss.

4. Vision recovery following chiasmal decompression

4.1. Recovery occurs in stages

Post-operative recovery of vision can range from no improvement to complete recovery. The rates of visual recovery reported following treatment for chiasmal compression vary dramatically (from 23 to 81%) based on the study population, visual parameters evaluated, treatment technique and nature of the tumors (Cohen et al., 1985; Ebersold et al., 1986; Findlay et al., 1983; Klauber et al., 1978; Laws et al., 1977; Lennerstrand, 1983; Peter and De Tribolet, 1995; Powell, 1995; Sullivan et al., 1991). A recent meta-analysis showed that the overall prevalence was 40.4% for complete recovery (95% CI: 34.8–46.3%) and 80.5% (95% CI: 77.7–83.6%) for partial recovery (Muskens et al., 2017).

Electrophysiological studies have demonstrated improvement in VEP amplitude occurring as early as 10 min (measured intra-operatively) after surgical decompression in some patients (Feinsod et al., 1976) (see section 5.5.4). Frisen reported a case of a patient who had an instant subjective vision recovery by drainage of a recurrent craniopharyngioma cyst (Frisen et al., 1976).

Improvement of visual function is most commonly reported within the first two weeks. Findlay et al. found that 50% of maximal recovery was achieved within ten days of surgical decompression, and 28% of the patients attained maximal recovery during this period (Findlay et al., 1983). Normalization of visual acuity and visual field was observed in a small proportion of patients with perichiasmal tumors within five to seven days (Gnanalingham et al., 2005; Kayan and Earl, 1975; Kerrison et al., 2000), and in 66% of patients with pituitary tumors within two weeks (Yoneoka et al., 2015). Similar early recovery has been reported in patients with pituitary apoplexy. Recovery in visual acuity and field began within 24 h of decompression in most cases, if surgery was performed early (Agrawal and Mahapatra, 2005; Seuk et al., 2011). Partial to complete recovery in visual field defect was observed within an average of 8 days (range 1–42 days) (Zaidi et al., 2016).

Retrospective observational studies where patient cohorts were followed up at various time points showed that recovery in visual field indices was continuous throughout the follow-up period (Dekkers et al., 2007; Gnanalingham et al., 2005; Goyal et al., 2013; Kerrison et al., 2000; Moon et al., 2011b). Kerrison et al. showed the greatest improvements in mean deviation occurred between visit 1 (surgery to week 1) and visit 2 (one to four months post-operatively) (Kerrison et al., 2000). Between visits 1 and 2, the overall mean deviation improved by 33% in the left eye, and 30% in the right eye. At both visits 1 and 2, the inferotemporal quadrants showed most improvement. Gnanalingham et al. followed patients with pituitary adenomas for up to five years (Gnanalingham et al., 2005). Although visual field recovery occurred in all quadrants, the superotemporal quadrants showed the greatest improvements, followed by inferotemporal and nasal quadrants. More than 50% of eventual recovery took place between three and six months.

We showed gradual recovery in mean deviation and pattern standard deviation during 9–15 post-operative months (Danesh-Meyer et al., 2015). In our study, 81% of eyes with normal RNFL thickness achieved a final mean deviation of better than −2 dB, while only 37% of eyes with thin RNFL (below the 5th percentile of normal values) achieved normal mean deviation (Danesh-Meyer et al., 2015). Final visual acuity was at least 6/12 in 98% of eyes with normal RNFL, compared to 88% of eyes with thin RNFL (Danesh-Meyer et al., 2015). Of the total amount of improvement approximately two-thirds of this occurred between the first post-operative visit (6–10 weeks) and the fifteen month time point. Modest and gradual improvement of visual fields has been documented to continue to occur years after decompression (Findlay et al., 1983; Gnanalingham et al., 2005; Kerrison et al., 2000; Powell, 1995; Rivoal et al., 2000; Sleep et al., 2003; Stark et al., 1999).

Prolactinomas are often decompressed using dopamine agonists, such as bromocriptine or cabergoline, before considering surgery. Dopamine agonists work by reducing the cell size and can shrink both micro and macroadenomas (Schlechte, 2007). Reduction in tumor size is relatively rapid with most reduction occurring in the first three months of treatment (Bevan et al., 1992). In a meta-analysis of 271 macroprolactinomas, 79% of the tumors shrunk by at least 25% in size with medical treatment (Bevan et al., 1992). Visual outcome following medical therapy is comparable to the surgical outcome. In some cases, dramatic improvement in visual field and/or acuity is seen within days of initiating dopamine agonist (Ivan et al., 2005; Tasan et al., 2015; Woodhouse et al., 1981). Within three months, normalization of visual field has been reported in 33–86% of patients (Corsello et al., 2003; Moraes et al., 2013; Shimon et al., 2007).

4.2. Proposed mechanism of recovery

Recovery of vision following chiasmal decompression is likely to take place in distinct but overlapping stages (Kerrison et al., 2000; McDonald, 1982). The temporal distinction between these stages of vision recovery remains incompletely defined.

4.2.1. Immediate recovery

The first early stage begins as soon as the compression is removed. Significant visual improvement often occurs at this early stage. The mechanism of this initial improvement in visual function is thought to be predominantly related to rapid reversal of conduction block. Only a few studies have evaluated this early recovery. As discussed above, detachment of the myelin loops at the paranodes has been shown to occur with compression that impairs transmission (Waxman and Swadlow, 1977). This detachment can be rapidly reversed following decompression which may contribute to the initial recovery of vision (Cottee et al., 2003).

A further explanation for early recovery of conduction is due to the reorganization of microtubules disorganized by the pressure (Cottee et al., 2003). In a rodent model of optic nerve compression, the pressure caused disruption of heavy neurofilaments with failure of both anterograde and retrograde axonal transport which was restituted at approximately two weeks (Hanke and Sabel, 2002). In a rat tibial nerve compression model, compression caused a disruption of microtubules that led to a functional deficit (Kitao et al., 1997). This resolved within three days following release of pressure.

In a more recent study using DTI, Hajiabadi et al. utilized intra-operative DTI to measure the distance between the optic tracts in patients undergoing decompression of pituitary adenomas (Hajiabadi et al., 2016). As the chiasmal compression was released intra-operatively, the DTI signals from the chiasmal crossing fibers appeared, reducing the distance between the two optic tracts on a coronal view (as measured by the fiber tractography images at a preset location). The majority of visual improvement occurred within the first week and slower and less improvement between one week and three months. Decreased distance between optic tracts correlated significantly with post-operative visual recovery. They concluded that the reduced

distance between the two optic tracts reflects release of conduction block with improved axoplasmic transportation.

4.2.2. The second stage of recovery

In the second stage, improved axoplasmic flow and remyelination contribute to sustained recovery over weeks to months. In the feline optic nerve compression model, remyelination coincided with the second stage of conduction recovery, occurring between 6 and 11 weeks after decompression. This was measured by electron microscopy measurement of myelin thickness and axon diameter (Clifford-Jones et al., 1985; Cottee et al., 2003). Remyelination continued up to 3 months after decompression. Other models of optic nerve injury also demonstrate this process of remyelination. In a rat model of optic nerve crush which damages around 85% of RGCs, retrograde/anterograde axonal transport and heavy neurofilament immunostaining reappeared 12 days after the initial injury, which correlated in time with recovery of visual performance and VEPs (Hanke and Sabel, 2002). Smith et al. studied CNS demyelination following an acute micro-injection of lysophosphatidyl choline in to the spinal cord (Smith et al., 1981). Their observations were that: demyelination occurred within 3 days and was complete by day 7; glial proliferation occurred days 7–10; and remyelination began on day 10 and was complete in the surviving axons by three months. Remyelination of damaged axons has also been observed in feline models of optic nerve compression and chemically induced demyelination (Clifford-Jones et al., 1980, 1985; Cottee et al., 2003; Jacobson et al., 1979).

Further understanding of the process of remyelination with chronic compression can be gained from considering experimental models of spinal cord compression. Harrison and McDonald utilized an experimental model of spinal cord compression in six cats at L1 level by resting a smooth tipped brass screw on the unopened dura for 3 h while monitoring somatosensory evoked responses (Harrison and McDonald, 1977). They demonstrated that even 3 h of transient spinal cord compression produced demyelination. Remyelination was seen at their earliest post-procedure time point of three weeks. The thickness of myelin around remyelinated axons increased gradually over months and even at their last time point of 18 months, many of the axons had thin remyelinated sheaths.

Paul et al. demonstrated evidence of remyelination in the optic tract within four weeks of surgical decompression of pituitary adenoma in humans using DTI (Paul et al., 2014). Pre-operatively, there was uniform increase in radial diffusivity (indicating increased demyelination) in the length of optic tract from the chiasm to the lateral geniculate nucleus. The patients had reduced contrast sensitivity and mostly temporal visual field defects which matched the fMRI-based retinotopic map. At four weeks following decompression, fractional anisotropy (measure of white matter tract integrity), mean diffusivity (measure of axonal membrane permeability) and radial diffusivity significantly improved in 93% of examined optic tracts, but did not fully recover to the healthy control level. Decrease in axial diffusivity (indicating axonal degeneration) was seen in the majority of the optic tracts post-operatively, although this was statistically non-significant. The degree of post-operative remyelination was positively correlated with visual outcome and normalization of fMRI retinotopic maps. This suggests that rapid regeneration of myelin in the human brain is a component of the normalization of cortical activity, and ultimately the recovery of sensory and cognitive function, after decompression (Paul et al., 2014).

4.2.3. The third stage of recovery

The third stage consists of a phase of delayed recovery occurring months to years after chiasmal decompression. The physiological basis of the third stage of recovery remains unknown. We postulate that it is likely to be slow remyelination (Schultz et al., 2017).

5. Predictive factors for visual recovery following chiasmal decompression

Visual dysfunction and recovery from chiasmal compression is a complex and heterogeneous process. Prediction of post-operative visual outcome requires knowledge of the quantity of irreversibly damaged neurons of the visual pathway.

As yet, there is no *in vivo* test which can differentiate permanently damaged axons from those with reversible injury, such as physiological conduction block and demyelination. This section discusses the prognostic strengths of various clinical parameters that have been tested as predictive factors for post-operative vision recovery.

5.1. Clinical examination

Clinical examination findings and patient characteristics are easily accessible but provide limited information about irreversible damage to the visual pathway.

5.1.1. Duration of symptoms

There are conflicting reports on the predictive power of pre-operative duration of symptoms in regards to post-operative visual outcome. Some studies found significant correlation between post-operative visual acuity or visual field, and the duration of symptoms (Cohen et al., 1985; Dutta et al., 2016; Grkovic and Davidovic, 2016; Jacob et al., 2009; Prieto et al., 2015; Sun et al., 2017a; Tokumaru et al., 2006), while others did not (Barzaghi et al., 2012; Findlay et al., 1983; Gnanalingham et al., 2005; Lennerstrand, 1983; Peter and De Tribolet, 1995; Powell, 1995; Rivoal et al., 2000; Sleep et al., 2003; Trobe et al., 1984). This is most likely related to a combination of factors including patient recall, whether visual impairment impacts central visual acuity, presence of hormonal symptoms and position of the tumor.

Individuals with pituitary apoplexy have a short duration of symptoms from hours to days, but do not always have a favourable visual outcome. The proportion of apoplexy patients who achieve full visual recovery varies from 31% to 100% (Barzaghi et al., 2012; Choudhry et al., 2012; Dutta et al., 2016; Randeva et al., 1999; Takeda et al., 2010). In general, recovery was more likely in those with mild pre-operative visual impairment, although there is significant variability (Agrawal and Mahapatra, 2005; Barzaghi et al., 2012; Dutta et al., 2016; Muthukumar et al., 2008; Parent, 1990). Some patients already showing evidence of improvement at presentation completely recovered without surgery (Ayuk et al., 2004). Taken together, duration of symptoms may influence, but cannot independently predict the final post-surgical visual outcome.

It has been suggested that the duration of symptoms may affect the rate of recovery, rather than the final visual outcome. Dutta et al. found that a short duration of symptoms was associated with increased likelihood of visual recovery in the early post-operative periods (Dutta et al., 2016). They found that 33.2% of patients with symptom duration less than 6 months showed visual acuity improvement at the immediate post-operative follow-up, while only 1.4% of those with symptom duration more than 1 year showed improvement during the same period. Those with symptom duration of more than 1 year showed gradual recovery over 12 months. In their study, the final visual outcome at 1 year was good irrespective of the duration of symptoms. Similarly, a recent large-scale observational study showed that prolonged duration of symptoms was correlated with decreased rate of recovery (Anik et al., 2018). Presumably, visual dysfunction sustained over a short period is more likely to be caused by reversible conduction block, and therefore recovers faster. Demyelination and axon degeneration sustained over a longer period may recover more slowly. However, patients are asymptomatic for an unknown and variable length of time. Furthermore, many factors influence whether patients notice visual impairment and accurately determining the duration of symptoms is not reliable.

5.1.2. Optic disc pallor

Since optic atrophy indicates RGC death, it is expected to be a strong negative prognostic factor for vision recovery. However, the studies that have evaluated the prognostic strength of optic nerve head pallor showed inconsistent findings. While many studies showed significant negative correlation between the degree of optic atrophy and post-operative improvement in visual acuity or visual field (Ho et al., 2015; Klauber et al., 1978; Lennerstrand, 1983; Monteiro et al., 2010b; Prieto et al., 2015; Trobe et al., 1984); other studies showed no or weak correlation (Gnanalingham et al., 2005; Peter and De Tribolet, 1995; Powell, 1995; Sullivan et al., 1991). Marcus et al. showed optic atrophy carried a poor prognosis only if the pre-operative visual acuity was worse than 6/12 (Marcus et al., 1991). This inconsistency may be explained by the highly subjective nature of grading of disc pallor and atrophy (see section 2.4.3. Optic atrophy).

5.1.3. Age, sex and endocrine status

Although one would expect young age to be a positive prognostic indicator, this is not clearly reflected in the studies to date. Some studies identified increased age as an independent negative prognostic factor for recovery (Barzaghi et al., 2012; Jacob et al., 2009; Rivoal et al., 2000; Sun et al., 2017a). A meta-analysis found a weighted mean difference of 12.32 years (95% Cl: −18.42 to −6.22, $p < 0.0001$) between groups which showed visual field improvements and those who did not (Sun et al., 2017a). Other studies, however, failed to show correlation between age and post-operative outcome (Dutta et al., 2016; Findlay et al., 1983; Gnanalingham et al., 2005; Grkovic and Davidovic, 2016; Lee et al., 2016; Marcus et al., 1991; Monteiro et al., 2010b; Sullivan et al., 1991). Sex and endocrine status of patients did not predict post-operative visual outcome (Barzaghi et al., 2012; Cohen et al., 1985; Lee et al., 2016; Monteiro et al., 2010b; Rivoal et al., 2000).

5.2. Visual acuity

There does not seem to be a consistent relationship between pre- and post-operative visual acuities amongst different studies. Patients with 6/6 vision pre-operatively are more likely to retain normal vision (Lennerstrand, 1983; Marcus et al., 1991; Prieto et al., 2015); better pre-operative visual acuities are correlated with increased likelihood of post-operative improvement (Barzaghi et al., 2012; Cohen et al., 1985; Dutta et al., 2016; Gnanalingham et al., 2005; Grkovic and Davidovic, 2016; Klauber et al., 1978; Trobe et al., 1984), and those with severely decreased visual acuity are less likely to improve although there is marked variability amongst studies (Dutta et al., 2016; Monteiro et al., 2010b; Peter and De Tribolet, 1995). Other studies showed that pre-operative visual acuity was not related to post-operative visual acuity or visual field (Powell, 1995; Sleep et al., 2003; Sullivan et al., 1991). Even patients with no-light perception vision achieved some improvement following decompression (Dutta et al., 2016). No multivariate analysis identified visual acuity as an independent predictive factor.

5.3. Perimetry

Pre-operative mean deviation has been positively correlated with recovery (Barzaghi et al., 2012; Findlay et al., 1983; Gnanalingham et al., 2005; Lee et al., 2016; Prieto et al., 2015; Sun et al., 2017a). Less than two quadrant involvement (any two quadrants) was a predictive factor for visual field recovery (Klauber et al., 1978). A multivariate analysis showed less than two quadrant involvement (any two quadrants) was an independent predictor of visual field recovery with an odds ratios of 8.244 ($p = 0.016$) (Yoneoka et al., 2015); on the other hand, other studies showed no correlation (Jacob et al., 2009; Powell, 1995; Sullivan et al., 1991). The post-operative outcome becomes unpredictable in the presence of extensive visual field loss, as some patients with severe visual field defects show marked improvement (Findlay et al., 1983). The likely reason that perimetry and visual acuity are variable predictive markers is that these functional tests do not differentiate between reversible and irreversible injury to the visual pathway.

5.4. Neuroimaging

A consistent finding among studies of chiasmal pathology is that larger tumors are associated with greater visual field loss pre-operatively (Ho et al., 2015; Lee et al., 2016; Monteiro et al., 2010b). While tumor size is associated with pre-operative visual morbidity, the relationship between tumor size and post-operative visual recovery is less clear.

A number of recent MRI-based studies have found a general trend that larger tumor size was predictive of poorer visual recovery (Anik et al., 2018; Barzaghi et al., 2012; Grkovic and Davidovic, 2016; Ho et al., 2015; Lee et al., 2016; Monteiro et al., 2010b). The assumption is that the size of the tumor may be a surrogate for other markers, such as time the tumor has been compressing the chiasm and the amount of axonal degeneration (Lee et al., 2016; Monteiro et al., 2010b). A further study measuring meningioma size using a mix of CT and MRI found that the bigger the tumor, the smaller the chance that the visual acuity would return to normal (Grkovic and Davidovic, 2016). Another study of 78 patients with pituitary adenomas found that the final visual outcome in patients with larger adenomas was poorer than that of patients with adenomas less than 20 mm in size (Ho et al., 2015).

In contrast, there are reports of poor association of tumor size with visual recovery, but for the most part these were older studies that did not employ modern imaging techniques. A study of patients with acromegaly and visual field defects identified 38 such patients between 1951 and 1996 (Rivoal et al., 2000). They found that the presence of suprasellar extension was unrelated to visual field at the final follow-up. Similarly, older studies using CT imaging in the 1970s and 80s to estimate tumor size, failed to find an association with post-operative visual outcome (Findlay et al., 1983; Hudson et al., 1991; Lennerstrand, 1983).

More recently, a study of 38 patients with pituitary tumors found no statistically significant difference in visual outcome related to size, but there was a trend to worse visual outcomes with larger tumors, raising the possibility the study was underpowered to detect a difference (Chabot et al., 2015). Finally, a study only looking at patients with giant pituitary adenomas, did not find an association with increasing size and worse visual prognosis (Chohan et al., 2016).

A limitation of reporting in this area relates to how studies report improvement. Although worse initial visual acuity may be associated with greater acuity improvement, in part this can be explained by the fact that a greater visual deficit provides a bigger opportunity for the vision to improve. An alternative method of reporting is to note percentages of recovery to a pre-set threshold, which provides information on rate of reaching a functional level of visual function, which is not biased by the original level of visual impairment. Finally, the length of follow up is critical; insufficiently long follow up will underestimate the true amount of recovery given late phase recovery is well documented.

Recently CE-FIESTA (contrast-enhanced fast imaging employing steady-state acquisition) MRI has been employed to predict visual outcome. The technique uses the T2 steady-state coherent imaging sequences. FIESTA signal is related to the ratio of T2 to T1, rather than T1-or T2-weighted MRI. CE-FIESTA provides high spatial and contrast resolution between CSF and solid structures, and is able to demonstrate fine anatomic details of cranial nerves (Sheth et al., 2009). CE-FIESTA hyperintense signals along the optic nerve have been associated with persistent visual impairment after decompression (Hisanaga et al., 2017; Watanabe et al., 2012). CE-FIESTA MRI also demonstrated kinking of the optic nerve at the optic canal orifice in patients with pituitary macroadenoma (Hisanaga et al., 2017). The angle of optic nerve kinking was an independent predictor of short-term post-

operative improvement in visual acuity and visual field, while other imaging parameters, such as tumor height, severity of chiasmal compression and signal hyperintensity, were not. The long-term consequences of CE-FIESTA abnormalities await confirmation in future larger-scale studies.

Several studies showed good results using DTI to predict the extent of vision recovery following decompression. DTI can be used as an *in vivo* measure of demyelination, axonal degeneration and fiber integrity. In a study by Paul et al., low pre-operative radial diffusivities (indicating a low degree of demyelination) in the optic tract correlated significantly with visual field improvement at four weeks, while axial diffusivities (measure of axonal degeneration) correlated weakly (Paul et al., 2014). The radial diffusivities decreased to normal values four weeks after decompression, further supporting that the high pre-operative radial diffusivities represented reversible demyelination. Anik et al. showed that low pre-operative fractional anisotropies (measure of white matter tract integrity) and high mean diffusivities (measure of axonal membrane permeability) were significantly correlated with poor visual outcome at six months (Anik et al., 2011). The patients with abnormal pre-operative DTI parameters had significantly longer duration of symptoms, compared to those with normal parameters. In a subsequent follow up study they assessed 200 patients and followed them up for three years with serial DTI. They found that the DTI parameters provided a good differentiation for which patients were likely to improve and those who were not (Anik et al., 2018). These findings indicate that DTI has the potential to detect reversible and irreversible changes in the visual pathway and therefore could be a reliable predictive indicator for vision recovery.

The variable predictive power of pre-operative neuroimaging may in part be explained by the poor correlation between macroscopic structural changes and functional loss. As described in section 2.4.1., tumors of equal size can produce varying degrees of visual impairment. One explanation for this is that the optic nerves may adapt to chronic compression by remyelination, giving rise to varying ratios of demyelinated and remyelinated fibers within a compressed nerve. In a feline model of optic nerve compression, remyelination occurred in the presence of the causative compressive lesion, restoring conduction to some extent (Clifford-Jones et al., 1980, 1985). In their model, the compressed nerves were composed of a mixture of demyelinated, partially demyelinated and remyelinated fibers after three weeks of compression. Anatomical parameters measured on CT or MRI scans do not provide information about the number of axons that will recover once decompressed.

5.5. Electrophysiological studies

5.5.1. VEP abnormalities in chiasmal compression

VEPs are electrical signals generated at the occipital cortex in response to visual stimuli, and reflect the integrity of the visual pathway. Chiasmal compression gives rise to the characteristic asymmetric distribution of VEPs in response to full-field stimuli (Holder, 1978). Chiasmal compression produces crossed asymmetry where the P100 is lateralized over the right hemisphere to the left eye stimulation, and lateralized over the left hemisphere to the right eye stimulation. Occasionally, post-chiasmal compression can give rise to uncrossed asymmetry where stimulation of either eye produces similar asymmetrical distribution across the two hemispheres. Brecelj et al. showed that almost all patients with chiasmal compression had abnormal VEP responses to temporal half-field stimulation (Brecelj, 1992; Brecelj et al., 1989, 1992). In chiasmal compression, non-recordable P100, significantly attenuated P100 waveforms, or delayed P100 are observed more commonly during temporal rather than nasal field stimulation (Brecelj, 1992; Brecelj et al., 1989, 1992). Large tumors are more likely to affect VEP recordings from both crossed and uncrossed fibers, whereas small tumors with mild compression mostly affect recordings from crossed fibers only (Brecelj et al., 1992).

VEPs are correlated with perimetry findings. The majority of patients with abnormal temporal half-field (crossed fibers) VEPs had temporal hemianopia, while those with abnormalities in the nasal and temporal half-field VEPs (crossed and uncrossed fibers) had more extensive visual field defects (Brecelj et al., 1992). All patients with absolute central visual field defects detected on Goldmann perimetry had reduction of the P100 amplitude (less than 1 μV) to full-field or half-field stimuli (Strucl et al., 1997).

We used multifocal VEPs to enable a more detailed spatial correlation between VEPs and areas of visual field defects. During multifocal VEP measurements, individual VEP responses from all areas of up to central 32° radius of the visual field are simultaneously recorded. The recorded multifocal VEPs can be topographically mapped and directly compared with visual field defects. In a cohort of patients with perichiasmal tumors, 87% of patients had abnormal visual field with an average mean deviation of -6.54 ± 7.43 dB, and 88% had abnormal multifocal VEP with a mean Accumap Severity Index of 81 ± 7.4 (Danesh-Meyer et al., 2006b). The mean deviation and the Accumap Severity Index were significantly correlated, and the most significant correlation was seen in the superotemporal quadrant ($r = 0.73$). Similarly, Qiao et al. showed that agreement between abnormal perimetry results and multifocal VEPs was 89% (Qiao et al., 2015); the agreement was highest in the temporal quadrant. In patients with bitemporal hemianopia, the multifocal VEP amplitudes were significantly reduced in regions corresponding to areas of visual field loss, and latency was unmeasurable in areas of severe visual field defect (Jayaraman et al., 2010). In eyes with post-decompression band atrophy, the temporal multifocal VEP P1 and N2 amplitudes were significantly reduced, but the latencies were preserved, indicating absence of active optic nerve compression (Sousa et al., 2017). Significant correlation was found between temporal visual field sensitivity loss and multifocal VEP N2 amplitudes. The most significant correlation was found between inferotemporal N2 amplitude and visual field sensitivity loss in the inferotemporal or superotemporal quadrants (both $p < 0.001$).

5.5.2. Electroretinography abnormalities in chiasmal compression

PERG reflects the function of RGCs. Optic nerve compression from perichiasmal tumors led to a reduction in the amplitudes of PERG N95 or b-wave (Holder, 1997; Kaufmann et al., 1986). Abnormal PERG in chiasmal compression indicates loss of functional RGCs, and PERG changes are more severe in eyes with band atrophy where irreversible retrograde RGC deaths have occurred. Pre-operatively, PERG is normal in over 70% of patients (Goyal et al., 2013; Kaufmann et al., 1986).

Early full-field or half-field PERG studies demonstrated significantly reduced P50 and N95 amplitudes in eyes with band atrophy, but failed to show correlation between temporal PERG amplitudes and temporal visual field loss (Cunha et al., 2008; Monteiro et al., 2009). In contrast, full-field or nasal hemifield PERG amplitudes correlated well with central or central-temporal visual field sensitivity (Monteiro et al., 2009), suggesting that the relationship between PERG and visual field sensitivity may be weak if visual field loss is severe. Multifocal PERG, however, has been shown to have a more consistent correlation between PERG and visual field loss in the temporal quadrants (Monteiro et al., 2012, 2013). In multifocal PERG, localized PERG responses are simultaneously recorded from multiple areas of the retina, and presented in a topographical map. All the P1 multifocal PERG amplitudes in the temporal sectors were significantly lower than those in the nasal sectors. The P1 multifocal PERG amplitudes in temporal sectors were significantly correlated with global visual field sensitivity and sensitivity in inferotemporal or superotemporal quadrants (Monteiro et al., 2012).

The photopic negative response (PhNR) of the light-adapted full-field electroretinogram is a negative wave that occurs after the photopic b-wave. The PhNR is thought to arise from the activity of RGCs. Patients with chiasmal compression had significantly reduced PhNR:b-wave ratio pre-operatively, and the ratio was correlated with the mean

deviation ($R^2 = 0.110$, $p = 0.026$) and the temporal visual field sensitivity ($R^2 = 0.286$, $p = 0.000$) (Moon et al., 2011a).

De Araujo et al. investigated the dysfunction of inner and outer retina layers in chiasmal compression using multifocal electroretinography (de Araujo et al., 2017). The main components of multifocal electroretinography reflect the activities of photoreceptors and bipolar cells, while the oscillatory potentials acquired by slow flash multifocal electroretinography represent inner and intermediate retinal layer function. The mean oscillatory potentials were significantly reduced in temporal and nasal hemiretinas, indicating functional abnormality at the level of the inner nuclear layer. The authors found an isolated reduction in multifocal electroretinography N1 amplitude in the inferonasal macula, suggesting photoreceptor dysfunction in that area.

5.5.3. Sensitivity of electrophysiological studies

The relationship between electrophysiological and perimetric changes in chiasmal compression is not straightforward. Many investigators reported abnormal VEP or PERG in the absence of measurable visual field loss or apparent chiasmal compression, with up to 45% of patients with normal visual fields having abnormal VEP recordings (Brecelj et al., 1989, 1992; Sadowski et al., 1995; Strucl et al., 1997). In 6 out of 8 eyes in patients with pituitary adenoma, retinotopic areas with normal VEP amplitudes and normal visual field showed prolonged latencies (Jayaraman et al., 2010). There have been case reports of suspected glaucoma with normal visual acuity, intraocular pressure, perimetry and RNFL thickness, but a rapid decline in PERG amplitudes, where the patient was then found to have a chiasmal tumor (Ventura et al., 2009). Furthermore, a small proportion of patients with only mild compression shown on CT had abnormal VEPs involving both crossed and uncrossed fibers (Brecelj et al., 1992).

On the other hand, normal VEPs have been reported in patients with clear visual field defects. A patient with superotemporal quadrantanopia showed normal symmetric VEP responses over the two hemispheres to full-field stimulation (Maitland et al., 1982). In our study, one-fifth of patients with abnormal visual fields had normal or borderline multifocal VEP (Danesh-Meyer et al., 2006b). Furthermore, PERG P50 amplitudes were still recordable in a patient with no light perception from long-standing chiasmal compression (Holder, 1997). The reason for this discrepancy is unknown but could be partially explained by inter-individual variation in VEP or PERG amplitudes (Hoffmann and Flechner, 2008).

5.5.4. Electrophysiological changes during post-operative recovery

Rapid electrophysiological recovery following chiasmal decompression has been described in several case reports. Feinsod et al. reported the results of intra-operative VEP monitoring in a patient with pituitary adenoma, 6/60 vision in the left eye, junctional scotoma and reduced color vision (Feinsod et al., 1976). Delayed latency and reduced amplitude of the N35 component were seen prior to surgical resection. These parameters improved 10 min after decompression, and returned to normal after 20 min. A day later, normalization of visual acuity, visual field and color vision was demonstrated. A patient with cystic craniopharyngioma who had loss of waveform morphology, markedly reduced VEP amplitudes and unrecordable latencies, showed a substantial improvement of VEP parameters within 3 h of relieving suprasellar pressure by aspiration of cystic fluid (Gutin et al., 1980). Moreover, in patients with intraorbital tumors where changes in gaze direction increased the degree of compression, immediate changes in both P100 amplitude and latency were observed depending on gaze position (Janaky and Benedek, 1992). These examples demonstrated conduction block which was rapidly reversible upon relief of compression.

In the early to intermediate post-operative stages, a varying degree of electrophysiological recovery has been reported. Patients with macroprolactinoma showed improvement in waveform morphology, increased temporal:nasal P100 amplitude ratio and development of previously absent temporal half-field waveforms within weeks of commencing bromocriptine therapy (Pullan et al., 1985). In a prospective study of 20 patients with perichiasmal tumors, the proportion of patients with normal PERG N2:P1 ratios increased from 77.5% preoperatively, to 85% one week after surgery, and to 87.5% six weeks after surgery (Goyal et al., 2013). The changes in mean N2:P1 ratio throughout the follow-up period, however, were non-significant. In another study, the PhNR:b-wave ratio remained reduced at one and three months after surgery, and then improved at six months, but these changes were again non-significant (Moon et al., 2011b). Lennerstrand showed VEPs remained impaired despite complete recovery of visual acuity and visual field during the six-month post-operative follow-up (Lennerstrand, 1983).

A delayed recovery in PERG and VEP has been observed in a few case reports of compressive optic neuropathy. In a young patient with optic nerve compression from contusion injury and severe loss of visual acuity, visual field, color vision and VEP, all parameters except for VEP normalized within three months (Janaky and Benedek, 1992). VEP did not return to normal until after one year. In a patient who had incomplete pituitary tumor resection, PERG amplitudes remained depressed for over three years despite normalization of RNFL thickness and visual field within four months (Ventura et al., 2009). A repeat MRI showed regrowth, not compressing the chiasm. After re-excision of the tumor, PERG amplitudes returned close to the baseline values. These findings raise a possibility of an unknown pathological process which causes reversible retrograde deterioration in RGC function, prior to the development of neuroimaging or visual field abnormalities.

5.5.5. Prognostic strength of electrophysiological studies

Some electrophysiological recordings have been shown to be predictive of post-operative visual recovery. The studies to date have been small, and the results somewhat variable. Goyal found no significant correlation between pre-operative PERG parameters and post-operative visual acuity and visual field (Goyal et al., 2013). In contrast, Parma found no association with acuity, but a good association with visual field parameters; an improvement in visual field defect was seen in 65% of patients with normal pre-operative N95:P50 ratio, and 27% of those with abnormal N95:P50 ratios (Parmar et al., 2000). Sadowski et al. identified reduced amplitude of pre-operative N95 as a negative predictor of visual field recovery (Sadowski et al., 1995). There is some preliminary work that suggests there may be a critical electrophysiological measure in order for functional recovery to occur (Raz et al., 2015; Ruther et al., 1998). Ruther et al. showed that PERG P50 amplitude greater than 2.5 μV and N95 amplitude greater than 3.5 μV were always associated with stable or improved visual field at post-operative days 5–10 (Ruther et al., 1998). Raz et al. reported a patient with chiasmal compression, bitemporal hemianopia, generalized RNFL thinning, decreased fractional anisotropy along the optic tract on DTI, and severely decreased amplitudes of multifocal VEP and prolonged latencies (Raz et al., 2015). Visual field recovery was only seen in quadrants where more than 50% of normally conducting fibers were identified, characterized by intact multifocal VEP latencies. This critical mass of normally conducting fibers was the best prognostic indicator for visual outcome two years after decompression.

Electrophysiological studies are sensitive measures of functionality of the anterior visual pathway and have shown potential in detecting subclinical changes when visual acuity and visual fields are normal. The existing evidence that electrophysiological studies are useful in predicting post-surgical visual outcome remains thin. An abnormal PERG or VEP recording can be due to either rapidly reversible conduction block or irreversible retrograde degeneration. We cannot yet accurately estimate the number of viable RGCs from PERG or VEP alone, and hence their prognostic value remains poor. There has been some evidence that PERG or VEP can provide a threshold value above which vision recovery will occur (Raz et al., 2015; Ruther et al., 1998), but

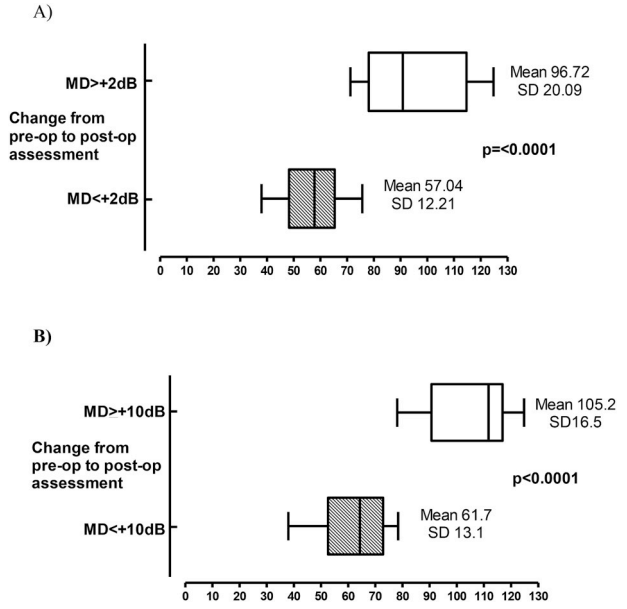

Fig. 5. Difference in RNFL thickness between the eyes in which MD improved by at least 2 dB (**A**) and at least 10 dB (**B**) from preoperative to postoperative assessments, among the eyes with the severe baseline VF defect of 10 dB or worse (Danesh-Meyer, 2008).

these studies were based on a very small number of patients. Further studies are required to validate the presence of threshold PERG or VEP value for visual recovery.

5.6. OCT

5.6.1. OCT of RNFL: correlation with functional studies

The first study to compare RNFL thickness with visual recovery post-operatively in patients with chiasmal compression was in 2006 (Danesh-Meyer et al., 2006a). Our study evaluated patients who had undergone surgery for chiasmal decompression and correlated the outcome of visual function (as measured by standard automated perimetry using Humphrey visual field analyzer) with post-operative RNFL thickness. We observed that pre-operative RNFL thickness correlated with post-operative visual function. Moreover, the correlation between RNFL and visual function strengthened as the time from surgical intervention increased (Danesh-Meyer et al., 2006a).

Our understanding of the mechanisms of visual loss in compressive optic neuropathies can explain the strengthening of the structure-function relationship as time from surgical intervention is increased. As discussed above, the mechanisms for visual loss include axoplasmic stasis, conduction block, demyelination and axonal destruction. Only the latter is thought to have an impact on the measured thickness of the RNFL. Axoplasmic stasis, conduction block and demyelination will contribute to the decrease in visual function but will not be measured by structural parameters such as RNFL thickness. Hence, during the early post-operative phases, the structure-function relationship is expected to be weaker as OCT will measure all surviving RGC axons regardless of their functional status. Immediate recovery is postulated to result from the removal of physiologic conduction block and restoration of signal conduction (Kayan and Earl, 1975).

Delayed recovery of visual function after compression of the optic nerve has been attributed to progressive remyelination of previously compressed axons that have undergone demyelination, or re-establishment of a vascular supply hampered by stretching by the tumor and consequent improvement of RGC function (Clifford-Jones et al., 1980; Jacobson et al., 1979; Kerrison et al., 2000; McDonald, 1982). As the interval from intervention increases, it is likely that the fate of the RGC is determined: either the dysfunctional RGCs recover, or they die. The relationship between structure and function strengthens as the proportion of RGCs that are damaged but not dead decreases. In other words, visual field testing measures defects produced by both dead and dysfunctional RGCs, whereas RNFL thickness is a measure of the surviving RGCs only. After the compression is relieved by surgical intervention, the visual field improves for those axons that were non-functional, and the anatomic measurements reflect the surviving axons. This suggests that visual sensitivity losses likely precede RGC death in compression syndromes, and psychophysical measures in this setting include a component of cell dysfunction as well as cell death. We demonstrated that OCT of RNFL predicts patients likely to demonstrate improvement of visual function if chiasmal compression is relieved (Danesh-Meyer et al., 2006a).

5.6.2. Prognostic strength of OCT of RNFL

To test the hypothesis that pre-operative RNFL thickness is predictive of post-operative recovery we undertook a prospective multicenter study (Danesh-Meyer et al., 2008). We observed that patients undergoing decompression for perichiasmal tumors display a variable range of pre-operative RNFL thickness ranging from normal (or slightly thicker) to dramatic loss of RNFL. Other investigators subsequently observed similar findings (Moon et al., 2011a, 2011b; Park et al., 2015; Yoneoka et al., 2015). The key observation was that pre-operative RNFL layer thickness has a variable correlation with pre-operative visual parameters such as visual acuity and visual field.

In contrast, the degree of reversibility of visual dysfunction with compression of the anterior visual pathway is related to the pre-operative RNFL thickness. In patients with normal RNFL thickness, visual function shows large improvements even in the presence of profound pre-operative visual field or acuity loss, whereas patients with thin RNFL and advanced visual field defect demonstrate significantly less improvement. We found that there is an increasing probability of improvement to near normal visual function (visual acuity better than 6/12 or mean deviation within 2 dB of normal) with increasing RNFL thickness up to approximately 85 μm, after which there is no additional benefit from thicker RNFL (Danesh-Meyer et al., 2008) (Fig. 5a and b). Eyes with 'thin' RNFL may still show some recovery, but the magnitude of the recovery is limited (Fig. 6).

In a subsequent study with a larger sample size, we reported the relationship between pre-operative RNFL thickness and visual outcome over a follow-up period of up to 15 months (Danesh-Meyer et al., 2015). Final visual acuity was shown to be well preserved in patients with pituitary adenomas, with only a minority demonstrating significant

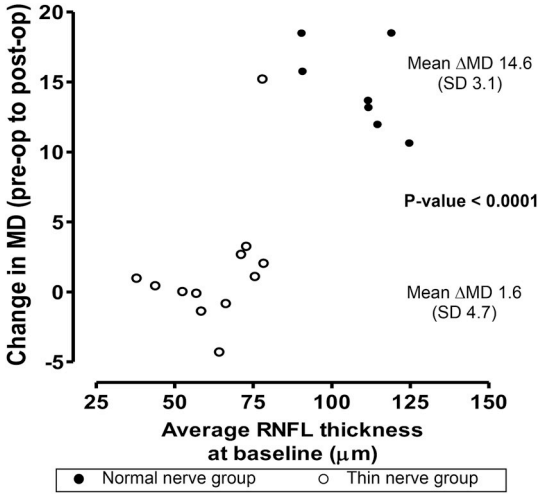

Fig. 6. Comparison of the magnitude of MD change from pre-op to post-op assessment in the Thin nerve group and Normal nerve group amongst the eyes with baseline MD ≤ -10dB (Danesh-Meyer, 2008).

visual impairment. Acuity of 6/9 or better at the final visit was achieved in 96% of eyes with normal RNFL thickness, and 90% of eyes with RNFL thinning. The majority of patients showed some improvement in their visual field defects following surgery, even those with thin pre-operative RNFL thickness. However, patients with a normal pre-operative OCT of the RNFL (> 80 μm in this study) improved to near normal visual field with a mean deviation of 0.9 dB. Those with normal RNFL thickness had significantly greater visual field improvement with 77.6% of eyes with normal RNFL compared to 21.7% of those with thin RNFL achieving a mean deviation of > 2.00 dB by six weeks after surgery (visit 2). This is useful information to provide counselling to patients regarding their potential visual field recovery following decompressive surgery.

The patients with normal RNFL thickness showed most improvement during the early post-operative stage (between surgery and 6 to 10 post-operative weeks), while those with RNFL thickness below the 5th percentile of normal values showed most improvement during the intermediate post-operative stage (between post-operative weeks 6–10 and post-operative months 9–15). At the last visit, 81% of eyes with normal RNFL thickness and 37.1% of eyes with thin RNFL achieved a mean deviation greater than −2 dB; 97.5% of eyes with normal RNFL thickness and 88.2% of eyes with thin RNFL achieved visual acuity of

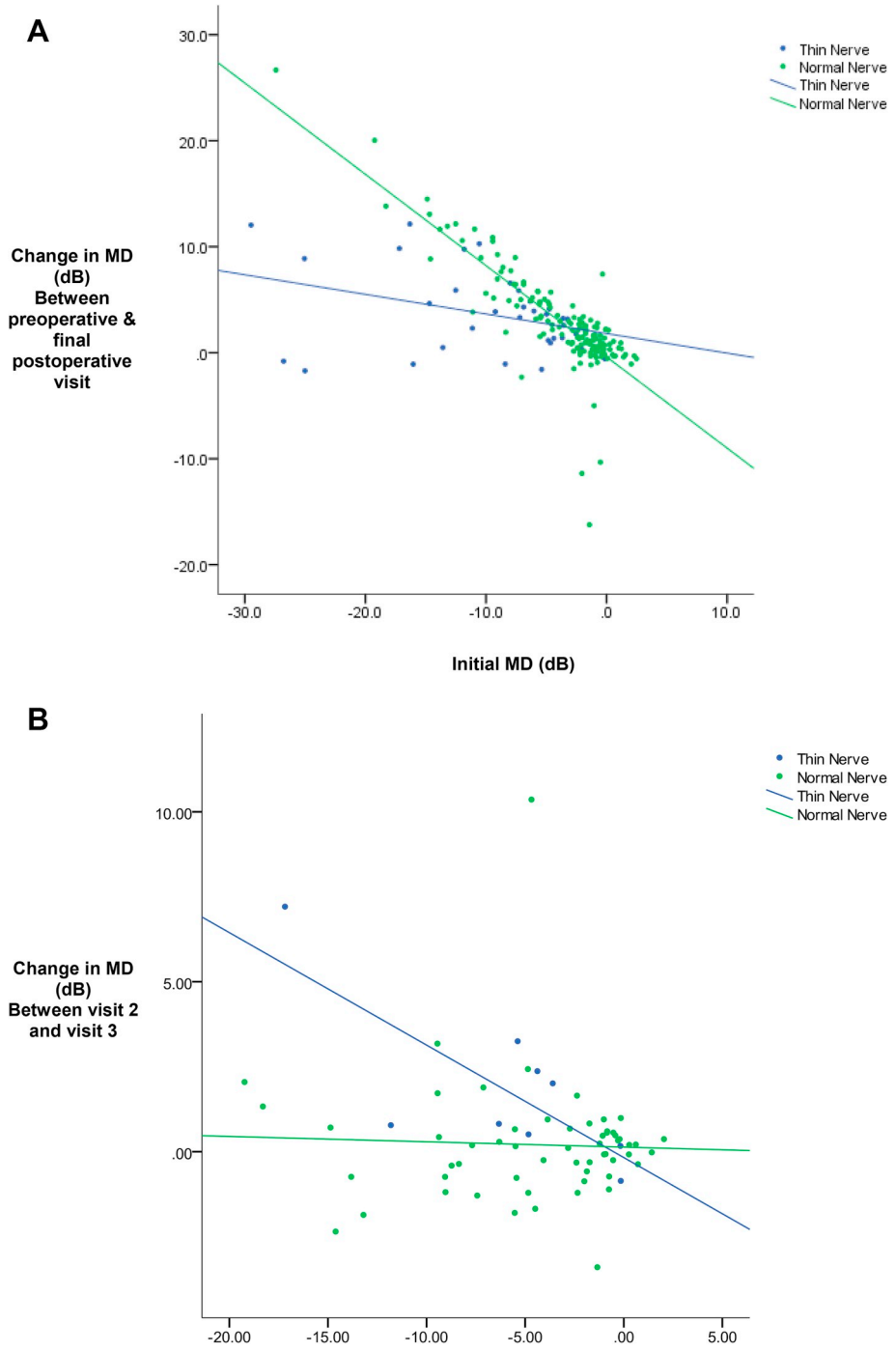

Fig. 7. a- Regression lines comparing change in MD between pre-operative baseline and final postoperative assessment (after 6 months) in the eyes belonging to the thin and normal nerve groups according to their baseline MD. $p < 0.001$. **b** - Regression lines comparing change in MD between immediate post-op (visit 2) and greater than six months (visit 3) assessments in the eyes belonging to the thin and normal nerve groups according to their baseline MD. $p < 0.001$.

6/12 or above. Patients with severe visual field defects with mean deviation worse than −10 dB showed a mean post-operative recovery of 12.4 ± 5.7 dB if they had normal RNFL thickness. Fig. 7 demonstrates that those with 'thick' RNFL continue to show improvement not only in the immediate post-operative phase (less than six weeks) but also beyond six months. While those with thin RNFL show some immediate improvement within six weeks, they are less likely to have ongoing improvement after six weeks.

Other investigators have made observations that have corroborated and extended our initial findings. Jacob et al. found that with follow-up duration of at least three months, a greater RNFL thickness increased the probability of complete recovery of the visual field defect, with the odds of complete recovery being multiplied by 1.29 for each increase in 1 μm of RNFL thickness. The effect was independent of age or duration of symptoms (Jacob et al., 2009). In the study by Park et al., patients with parachiasmal meningioma did not achieve visual improvement at all if the average RNFL thickness was below the 5th percentile of normal values (pre-operative mean deviation of −18.1 dB to −21.2 dB at six months, and −19.1 dB at one year; pre-operative visual acuity of 0.3 at six months and 0.4 at one year) (Park et al., 2015). More than 95% of patients with normal average RNFL thickness, however, showed post-operative improvement (pre-operative mean deviation of −5.9 dB to −2.8 dB at six months, and −1.1 dB at one year; pre-operative visual acuity of 0.6–0.9 at six months and one year). Loo et al. evaluated patients who had either surgery and/or radiation therapy for anterior pathway meningioma and found that patients with a thin RNFL were less likely to experience significant visual improvement after treatment (Loo et al., 2013).

A number of studies have published odds ratios of vision recovery based on OCT RNFL measurements. A recent meta-analysis showed a pooled odds ratio of 15.61 (95% CI: 4.09–59.61) for vision recovery in patients with normal RNFL thickness, compared to those with thin RNFL (Zhang et al., 2017). A multivariate analysis identified normal RNFL as an independent predictor of visual field recovery with an odds ratio of 62.137 ($p < 0.001$) (Yoneoka et al., 2015). In a cohort of Korean patients with pituitary adenoma, multiple logistic regression analysis showed that worse pre-operative visual field defect ($p = 0.018$), more severe MRI compression ($p = 0.009$), and inferior RNFL thinning ($p = 0.011$) were significantly associated with poorer visual outcome (Lee et al., 2016). The authors used these parameters to construct a nomogram which allowed prediction of visual field recovery. The area beneath the receiver operating characteristics curve was 0.84. RNFL parameters have also been used to predict macroscopic structural restoration of the optic chiasm (Yoneoka et al., 2015). Preserved RNFL thickness was associated with increased likelihood of restoring chiasmal symmetry after decompression. This implies that the compressed chiasm can restore morphological symmetry if the RNFL thickness is intact.

5.6.3. Comparison of OCT RNFL to electrophysiological tests

Electrophysiological tests have been shown to have some prognostic value. Both amplitude and the velocity of VEP are decreased in compressive optic neuropathies. Even patients with profound decreases in VEP may show complete recovery of VEP within minutes of decompression, suggesting that one mechanism for the depressed VEP is nerve conduction block relieved by surgical intervention (Feinsod et al., 1976; Gutin et al., 1980; Lewis et al., 1931). However, electrophysiology does not differentiate between decrease in visual function due to reversible factors, such as conduction block, and irreversible factors, such as retrograde RGC degeneration (Brecelj, 1992; Janaky and Benedek, 1992; Pizzorusso et al., 1997; Siliprandi et al., 1988). In addition, delays in latency in the VEP recording may occur in retinal dysfunction and cannot be considered pathognomonic of optic nerve disease (Holder, 2004). The PERG, another objective test of retinal function, originates from the inner retinal layers and provides an assessment of RGC function (Holder, 1987; Maffei et al., 1985; Ruther et al., 1998). Like the VEP, it requires complex equipment, electrodes that are placed on the eye, and a relatively time-consuming test procedure. PERG has also been investigated as a prognostic indicator (Parmar et al., 2000). Although the chance of visual field improvement after surgery is greater in those eyes with a normal PERG, 34% of such eyes showed deterioration or no change in visual field, indicating that PERG was not able to predict vision recovery.

5.6.4. Degree and pattern of thinning in chiasmal compression

Clinically, patients with chiasmal compression display the classic band (or bowtie) atrophy with horizontal pallor and preservation of the RNFL at the superior and inferior poles of the optic nerve head. This is because the RGC axons from the nasal hemiretinas (which cross at the chiasm) enter the disc temporally (papillomacular bundle) and nasally, while the uncrossed fibers which originate in the temporal hemiretina enter the optic nerve through the superior and inferior arcuate fiber bundles. Therefore, on ophthalmoscopy, pallor appears predominantly on the nasal and temporal sides of the optic disc. This pattern has been corroborated on OCT by RNFL assessment at the disc with temporal and nasal RNFL showing significant thinning.

However, several investigators have demonstrated that RNFL thinning actually occurs diffusely in all sectors, even in patients who had strict bitemporal hemianopic visual field loss (Danesh-Meyer et al., 2006a; Kanamori et al., 2004; Mikelberg and Yidegiligne, 1993; Monteiro et al., 2004; Moon et al., 2011b). The generalized thinning of the RNFL may be explained by the fact that every clock hour of the optic disc receives crossing fibers; even the temporal side of the disc receives fibers from the retina between the vertical meridian through the fovea and the disc. Mikelberg suggested that some RGC axons from the nasal retina penetrate the superior and inferior sectors of the disc (Mikelberg and Yidegiligne, 1993). They found that although the loss of nerve fibers in eyes with band atrophy occurs predominantly in the nasal and temporal segments, the superior and inferior areas of the optic disc lose approximately 50% of their fibers. This suggests that although compressive lesions of the chiasm primarily affect the crossing fibers, they also affect noncrossing fibers.

In terms of sectoral changes, the strongest correlations are found between temporal disc sectors and temporal visual field mean deviation (Danesh-Meyer et al., 2006a, 2015; Jacob et al., 2009; Moon et al., 2011b). The temporal RNFL also shows the strongest correlation with the corresponding central visual field as well as with central visual acuity and color vision. The nasal RNFL thickness does not seem to show as strong a correlation to the corresponding temporal visual field defect (Danesh-Meyer et al., 2006a; Johansson and Lindblom, 2009). The nasal hemiretina may have structural redundancy, or the fibers entering the disc at the temporal quadrant may be more vulnerable to compressive injury than those from the nasal retina.

In terms of prognostic value, temporal RNFL thickness shows the strongest correlation to baseline mean deviation (Danesh-Meyer et al., 2008, 2015; Moon et al., 2011a). In our studies, patients with normal pre-operative visual field had thicker temporal RNFL at visit 3 than those who had pre-operative visual field defect but who improved to within normal limits after surgery. This suggests that there is some loss of temporal RNFL even in patients who achieve complete recovery of mean deviation (Danesh-Meyer et al., 2015).

It is intriguing that some relationships that would have been expected to be strong were not. For example, the nasal RNFL did not show a strong correlation to the corresponding temporal sectors. This finding may be due in part to the smaller range of visual field defects in these sectors, as they all tended to be significantly abnormal. Also, the nasal visual field sectors did not show any significant correlation to the corresponding temporal optic disc sectors. Although we identified thinning in the superior and inferior RNFL of approximately 33%, the SITA-standard visual field test identified only mild abnormalities in the corresponding nasal sectors with no nasal sector showing a mean deviation of greater than 4.8 dB. This poor correlation may be due to the

limitation of white-on-white perimetry to identify early abnormalities in the visual field. Studies have shown that short-wavelength automated perimetry and frequency doubling technology have shown closer agreement with structural assessments in glaucomatous optic neuropathy. Further research comparing structural parameters with other psychophysical tests of visual function may demonstrate stronger correlations for compressive optic neuropathies.

5.6.4.1. Atypical results

5.6.4.1.1. Poor recovery despite normal RNFL. There is a cohort of patients with relatively normal RNFL who do not recover normal vision and have no history of intra-operative complications. There are several possible explanations. One possibility is incomplete or faulty remyelination following surgery. Experimental chronic compression of the optic nerve in cats demonstrated evidence of demyelination within a week of compression and subsequent remyelination. However, the reconstructed myelin sheaths were thinner than normal, with reduced intranodal distances (Harrison and McDonald, 1977). Even at 18 months after spinal cord compression, remyelinated fibers exhibited inappropriately thin myelin sheaths. Hence, although such remyelination may be associated with restored conduction of action potentials and recovery of visual function it remains unknown whether remyelination is capable of restoring the ability of previously demyelinated central fibers to impulse at physiological frequencies (Clifford-Jones et al., 1980; Kaufmann et al., 1986). Alternatively, microsurgical trauma may result in damage to the axons and influence visual recovery, which clearly would have not been detected by the pre-operative RNFL measurement. In our long-term follow-up study, we observed that generally patients who showed minimal improvement within the first six weeks did not show significant improvement (greater than 5 dB from pre-operative baseline) in the following months, although there was a small subset of patients who showed delayed recovery. However, generally, this recovery was less than 5 dB (unpublished data). This small subset would support the hypothesis of delayed remyelination.

5.6.4.1.2. Increase in RNFL thickness following surgery. We found there was a modest (1%) increase in average RNFL thickness after surgery, and that it was more marked in patients who had pre-operatively thin RNFL (below 5th percentile, average RNFL thickness 67.4 μm) (Danesh-Meyer et al., 2008). This study was the first to suggest an anatomically reversible injury that parallels the functional reversibility in chiasmal compression. This was corroborated in our 2015 study with the average RNFL thickness initially showing a slight decrease (4.1%) within the first six weeks following surgery but then increased (4.4%) between visits after three months. Conversely, patients who made good visual field recoveries tended to show greater (12.5%) increase in RNFL thickness (Danesh-Meyer et al., 2015). This anatomic recovery has also been described as occurring in the late post-operative stages (Moon et al., 2011b). It may be that RGCs whose axons are injured at the chiasmal area undergo an initial phase of reversible injury before axon and cell body loss that involves individual axon thinning. After removal of the chiasmal lesions, the slight thickening of the RNFL may result from restoration of normal axon diameter in these RGCs.

5.6.4.1.3. Normal visual field despite a significantly thin RNFL. A small cohort (15%) of our patients show normal standard automated visual field test results with thin RNFLs (below 5th percentile, average RNFL thickness 67.4 μm). This may be analogous to the well-known pre-perimetric glaucoma. Our study was the first to suggest that damage to the RGC axons may occur before identifiable visual field loss in patients with compressive optic neuropathy (pre-perimetric compressive optic neuropathy) (Danesh-Meyer et al., 2008). This is an area that requires further study and verification.

5.6.4.2. long-term changes in RNFL. Following decompression surgery, the RNFL may continue to thin despite recovery in visual field. In one study, the average, superior and inferior RNFL thicknesses (but not the nasal quadrant thickness) showed ongoing reduction during the first six months after decompression (Lee et al., 2016). In another cohort of patients, RNFL thinning progressed in all quadrants during the first three post-operative months (Moon et al., 2011b). The difference from the pre-operative RNFL was statistically significant in all quadrants except the temporal quadrant. Of note, the average RNFL thickness increased from 74.78 μm to 76.89 μm ($p = 0.03$) after three months of follow-up. Our 2015 study revealed a similar trend; we found that the average RNFL thickness decreased by 4.1% between pre-operative and first post-operative visits (6–10 weeks), and then increased by 4.4% between first and second post-operative visits (9–15 months) (Danesh-Meyer et al., 2015).

The post-operative loss of RNFL thickness does not parallel the

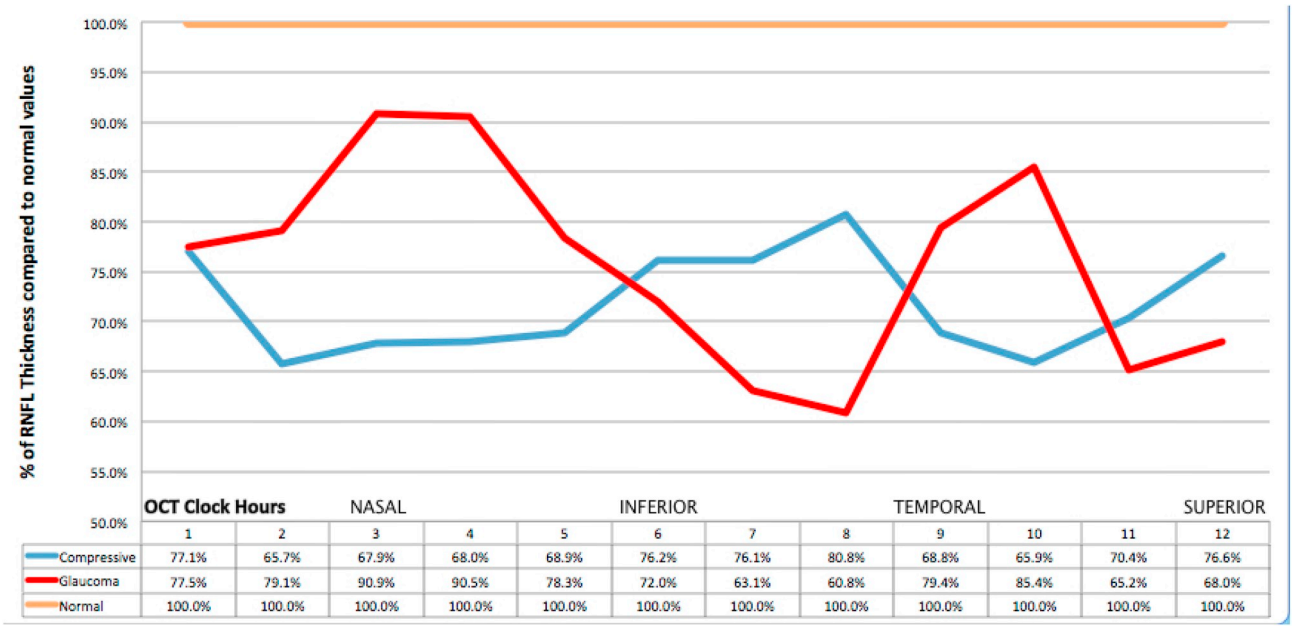

Fig. 8. Comparison of RNFL thickness of the CON and OAG groups when compared to normal according to clock hours (Danesh-Meyer, 2014).

changes in function observed following surgery. Recovery in visual function starts immediately after decompression. This difference may be explained by the status of function of the RGCs: the population of unaffected RGC axons will maintain stable RNFL thickness; those that have undergone atrophy are also stable, but the population of cells that are dysfunctional still have an undetermined fate. There will be a population of this latter cell type that will recover complete or near complete function. These RGCs explain the recovery of visual acuity and visual function that is observed. The RGC axons of this population may explain the increased thickness that is observed to occur weeks to months after surgery. One possibility is restoration of the original axonal diameter upon removal of compression. Axonal shrinkage has been observed during initial phases of reversible injury in experimental glaucoma models (Morgan, 2002). In chiasmal compression, similar axonal shrinkage may occur and then recover following decompression. On the other hand, there will be a population of RGC axons that are dysfunctional but will continue to die despite decompression, either as a result of surgical trauma or because the cells were already committed to death. These axons with irreversible injury may continue to show retrograde degeneration, thereby reducing the RNFL thickness.

5.6.5. Comparison of compressive optic neuropathy to glaucoma

Although compressive optic neuropathy produces characteristic changes in the optic nerve head, there is often a significant overlap with the appearance of other optic neuropathies, in particular glaucoma. One of the challenging clinical dilemmas is differentiating between glaucomatous and non-glaucomatous 'cupping' in relation to compressive lesions. The similarities that have been observed between compressive and glaucomatous optic neuropathies include enlargement of the cup and thinning of the RNFL. Bianchi-Marzoli et al. measured the cup:disc ratio from fundus photographs and showed that the median cup:disc area in patients with compressive lesions is significantly greater than in age-matched controls (Bianchi-Marzoli et al., 1995). A large retrospective study using fundus color photography, identified that patients with perisellar tumors showed changes in the optic nerve head that consisted of abnormal rim shape and failure to obey the ISNT rule (Qu et al., 2011). However, their findings were subtle; for example, a vertical cup:disc ratio of 0.47 ± 0.14 compared with normal discs of 0.44 ± 0.12. This suggests that there is a significant overlap in the optic nerve head morphology between glaucomatous patients and those with chiasmal compression.

However, despite this significant overlap, there are identifiable differences between 'cupping' or excavation of the optic nerve head in glaucoma and chiasmal compression. We have shown that OCT may assist in differentiating the pattern of optic nerve morphology between these two conditions. Although both compressive optic neuropathy and open angle glaucoma discs show enlargement of the cup and thinning of the RNFL, compressive optic neuropathies demonstrate proportionally more thinning nasally and temporally compared with open angle glaucoma, whereas the inferior RNFL was thinner in glaucomatous eyes when the level of visual field sensitivity damage was adjusted (Fig. 8). The OCT 3 o'clock hour seems to have a good discriminating power between glaucomatous and compressive optic neuropathies (Fig. 9). In terms of cup volume and depth, both optic neuropathies result in larger and deeper cups than normal discs. However, the cup depth in compressive discs is significantly shallower than in open angle glaucoma discs. Likewise, we identified that mean vertical cup:disc ratio was 0.48 for compressive patients while controls were 0.44 using the Heidelberg Retinal Tomograph, and 0.6 for compressive optic neuropathy compared with 0.4 for controls with spectral domain OCT (Danesh-Meyer et al., 2014). The preferential thinning of the nasal and temporal RNFL with compressive lesions has also been demonstrated with OCT assessments by other investigators (Danesh-Meyer et al., 2006a; Monteiro et al., 2010a).

The differences in RNFL thinning between glaucoma and chiasmal syndromes derive from the location of injury, the type of injury, and/or its chronicity. Current evidence suggests that the major site of damage in glaucoma is at the level of the optic nerve head/lamina cribrosa with the superior and inferior poles being the most susceptible sites. In chiasmal compression, the axons that are closest to the expanding mass are those crossing from the nasal hemiretina. The temporal hemiretinal fibers become involved when the tumor enlarges and affects the

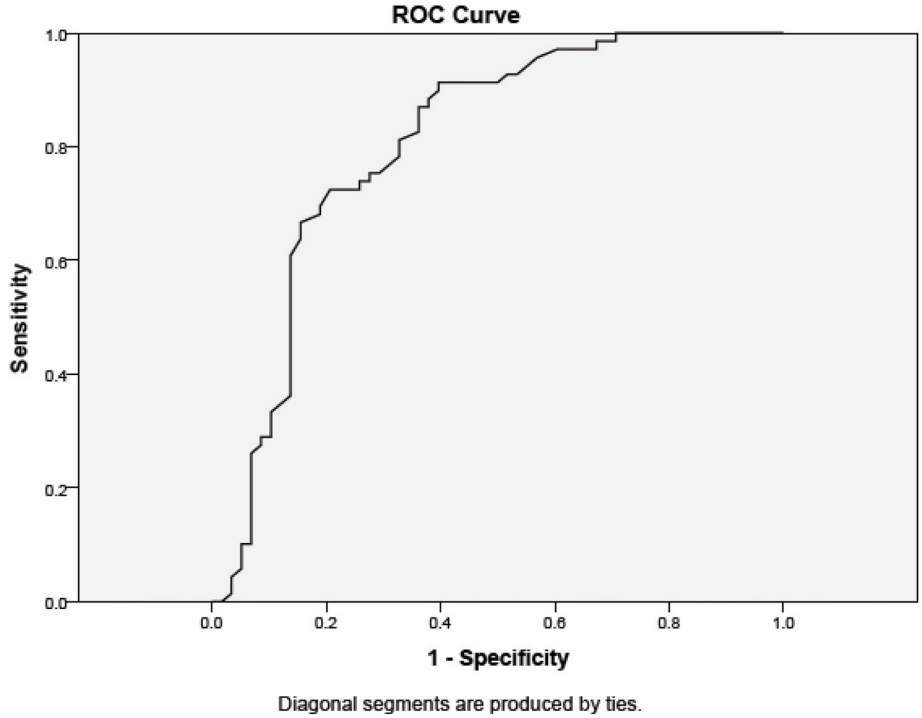

Fig. 9. Receiver operator curves for OCT clock hours demonstrates that the Area Under the Curve of the OCT 3 o'clock hour has very good sensitivity and specificty for discriminating OAG discs from chiasmal compression (Danesh-Meyer, 2014).

noncrossing fibers as discussed above.

Several theories have been postulated to explain the morphologic changes of the optic nerve head in compressive optic neuropathy. Qu et al. proposed that excavation in compressive lesions may occur when the trans-lamina cribrosa pressure gradient increases (Qu et al., 2011). A tumor that occludes the optic canal results in collapse of the CSF space, decreasing the CSF pressure and consequently increasing the pressure gradient. Other studies have supported the potential differences in CSF gradient as a mechanism for excavation of the optic nerve head (Morgan et al., 1995; Ren et al., 2010). Histopathologic assessment of a patient with excavation of the optic disc cup that resembled glaucoma demonstrated that change was caused by axonal loss, with anterograde degeneration, and secondary collapse of glial support tissue resembling glaucomatous changes (Portney and Roth, 1977).

5.6.6. OCT of macula

Macular OCT has been explored as a means of quantifying neuronal loss, as the RGC layer is thickest at the macula, making up of more than a third of total macular thickness (Galetta et al., 2011), and the RGC cell bodies are 10–20 times larger than the diameter of their axons (Ishikawa et al., 2005). The ganglion cell complex (GCC) includes the RNFL, cell bodies of macular ganglion cells, and axons and dendrites within the inner plexiform layer. GCC thickness measured by OCT is the distance from the internal limiting membrane to the outer boundary of the inner plexiform layer (Tan et al., 2009).

The pre-operative average GCC thickness has been found to be significantly reduced compared to healthy normal eyes (Danesh-Meyer et al., 2015; Moon et al., 2011a, 2011b; Ohkubo et al., 2012; Sun et al., 2017b; Tieger et al., 2017; Yoneoka et al., 2015). In addition, the thicknesses of total macula, macular RNFL and GCC were all significantly reduced in eyes with long-standing temporal hemianopia and band atrophy, compared to healthy normal eyes (Monteiro et al., 2009, 2010a, 2013, 2014; Moura et al., 2007; Sousa et al., 2017). Most studies identified the nasal macula as the most severely affected area. In the presence of visual field defect other than bitemporal hemianopia, different patterns of GCC thinning were observed. For example, a patient with a junctional scotoma showed generalized GCC thinning, and a patient with an inferior altitudinal defect showed superior GCC thinning (Tieger et al., 2017).

Binasal GCC thinning has been identified to occur in the presence of bitemporal visual field defects but normal RNFL thickness (Fig. 10). Tieger et al. identified in their study population that macular OCT demonstrated binasal loss in patients with mild or no visual field defects (Tieger et al., 2017). This suggests that GCC analysis may detect early or mild chiasmal compression and may have relatively more sensitivity than RNFL analysis. Furthermore, it also has been reported that GCC analysis may demonstrate thinning when the visual field is relatively stable suggesting that structural changes may precede functional change in compressive lesions. This concept requires further investigation (Monteiro, 2018).

Pre-operatively, the GCC parameters were significantly correlated with the PhNR:b-wave ratio, mean deviation and temporal visual field sensitivity, and this correlation was maintained until six months after surgery (Moon et al., 2011b). The inferotemporal macula quadrant was spared, which correlated with preserved nasal visual field (Tieger et al., 2017).

Similar to the post-operative peripapillary RNFL thickness changes, there was a significant post-operative reduction in the GCC areas three months after decompression; 0.223 to 0.208 mm^2 in horizontal scans ($p = 0.019$), and 0.234 to 0.219 mm^2 of average values ($p = 0.012$) (Moon et al., 2011b). The average values improved at six months (0.209–0.215 mm^2, $p = 0.024$) in a subset of patients.

The limitation of RNFL quadrant analysis is that all disc segments except for the nasal quadrant receive fibers from both temporal and

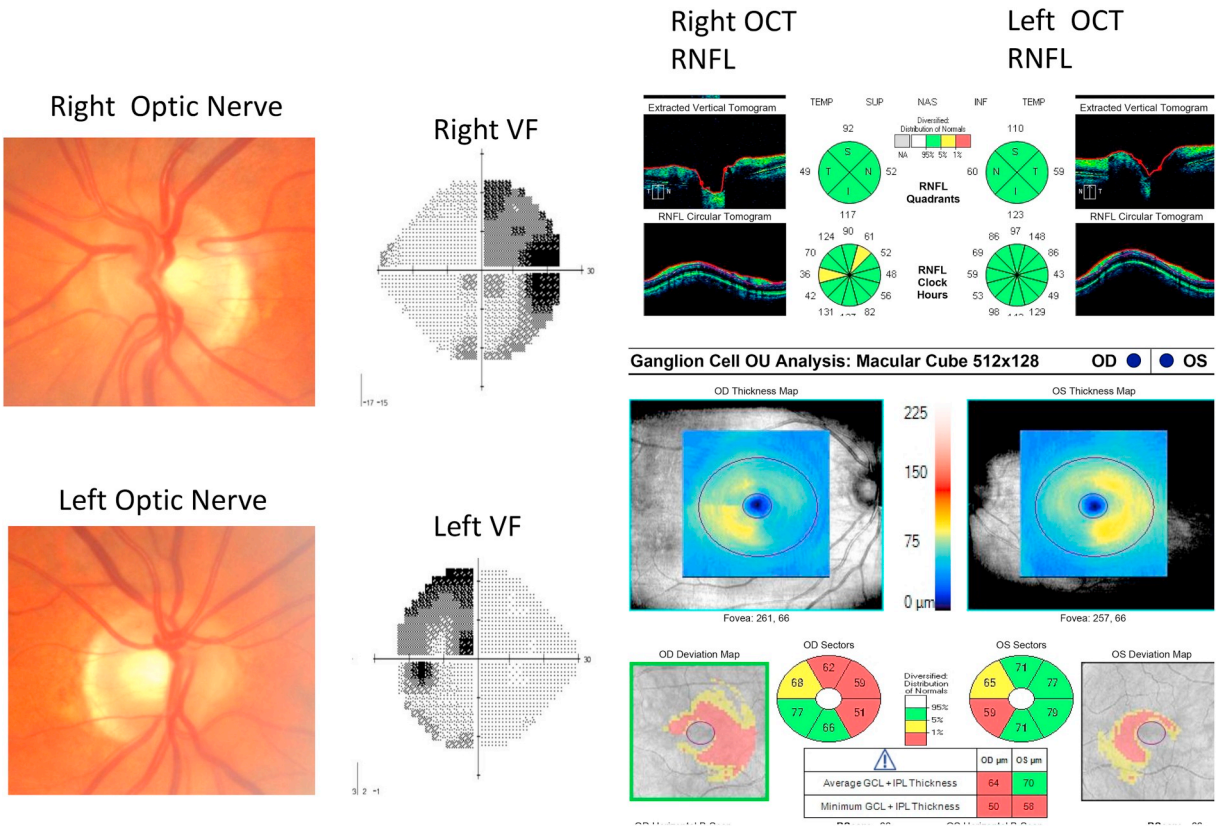

Fig. 10. Patient wit normal appearing optic nerves and OCT RNFL thickness. However, visual field test demonstrates a bitemporal hemianopia and ganglion cell layer thickness shows corresponding binasal loss.

nasal hemiretinas. The RNFLs in superior, inferior and temporal quadrants are likely composed of fibers from multiple areas of the retina. The macular quadrants, on the other hand, correspond directly to areas of visual field, and GCC thinning is expected to match the pattern of visual field defects more consistently than RNFL thinning. Indeed, a number of studies found a strong statistically significant correlation between the thickness of nasal macular quadrants and functional loss in the temporal visual field in patients with band atrophy. The inferonasal macula quadrant showed the strongest correlation with superotemporal visual field sensitivity (de Araujo et al., 2017; Monteiro et al., 2010a). Moura et al. found the strongest correlation between total macular thickness at the superonasal quadrant and inferotemporal visual field defect measured in both decibels and 1/Lambert (Molitch, 2002; Moura et al., 2007, 2010). The temporal multifocal VEP amplitudes (Sousa et al., 2017), multifocal PERG P1 amplitudes (Monteiro et al., 2013), multifocal electroretinography N1 amplitudes and oscillatory potentials (de Araujo et al., 2017) were significantly reduced in the thinned nasal macula.

Using the high resolution Fourier Domain OCT, two investigators found that the outer retina layers were significantly thickened in eyes with band atrophy (de Araujo et al., 2017; Monteiro et al., 2014). Monteiro et al. found that inner nuclear layers were significantly thickened compared to controls, and there were inner nuclear layer microcysts in 21.2% of the eyes (Monteiro et al., 2014). De Araujo et al. also found increased thicknesses of the inner nuclear layer, outer plexiform layer and photoreceptor layer in the nasal macula (de Araujo et al., 2017). In their study, the thicknesses of the nasal outer retina layers were negatively correlated with temporal visual field sensitivity. Furthermore, the inner nuclear layer thickness in the superonasal quadrant showed positive correlation with the amplitudes of oscillatory potentials (which represent the function of inner and intermediate retinal layers). However, Montiero et al. interestingly observed that the microcysts were limited to the nasal side of the macula, corresponding to the area of the worse visual field defect (temporal). Interestingly, the same investigators also demonstrated that the inner nuclear layer thickness was greatest in the nasal macula with the most axonal loss. The cause of microcyst formation and inner nuclear layer thickening in the nasal macula is unknown. It may represent a reactive process in response to retrograde axon degeneration (Abegg et al., 2014). Alternatively, it may represent retrograde transsynaptic degeneration (Monteiro et al., 2014).

5.6.7. Prognostic strength of OCT of macula

GCC thinning is thought to reflect the loss of RGCs. Some studies found OCT macular parameters a better predictor of post-operative visual field recovery than RNFL thicknesses (Moon et al., 2011a, 2011b; Tieger et al., 2017). Pre-operative average GCC thickness was significantly correlated with post-operative visual field mean deviation (Ohkubo et al., 2012; Tieger et al., 2017). Ohkubo et al. found that focal loss volume (the sum of losses in regions where there was significant focal loss) was significantly correlated with post-operative visual field loss (Ohkubo et al., 2012). Even if there was profound visual field loss, complete or near complete visual recovery occurred if GCC thickness was intact (Moon et al., 2011b; Ohkubo et al., 2012). This implies that profound visual field deficits occurred via reversible conduction block in the affected patients. Conversely, GCC analysis revealed significant thinning in the absence of obvious functional loss (Cennamo et al., 2015; Tieger et al., 2017; Yum et al., 2016). Post-operative normalization of visual field has been observed despite persistent GCC thinning (Tieger et al., 2017).

A few studies reported cases of subclinical macular involvement not detected on routine clinical examination. Gutowski et al. demonstrated reduced chromatic, luminance and temporal sensitivities in response to foveally-presented flash stimuli (Gutowski et al., 1997). All 11 patients had suprasellar extension of the tumor on neuroimaging and normal visual acuity and visual fields. Porciati et al. showed that contrast sensitivity to parvocellular pathway stimuli were frequently reduced in asymptomatic patients with normal visual acuity and field and pituitary adenomas not involving the chiasm (Porciatti et al., 1999). A case report by Romano et al. described a patient with pituitary adenoma with suprasellar extension, peripheral visual field defects and intact central vision (Romano et al., 2010). Microperimetry subtending a radius of 6° (white stimuli, Goldmann III, 200 ms) demonstrated loss of sensitivity in the right eye respecting the vertical meridian (visual field sensitivity 3.4 dB in the right eye versus 19.42 dB in the left eye). These studies indicate there may be an unknown mechanism other than mechanical compression leading to the subclinical functional abnormalities in the macula. It remains to be answered whether this subclinical functional loss can be correlated with GCC thinning.

5.6.8. OCT angiography

OCT angiography allows evaluation of perfusion of both the macula and peripapillary retinal capillaries. In a small group of four patients with persistent post-decompression visual field defects, reduced peripapillary vessel density has been demonstrated in the areas corresponding to visual field defects (Higashiyama et al., 2016). The reduced peripapillary vessel density measured by OCT angiography likely represents atrophic changes and loss of tissue perfusion following permanent loss of RGCs. This is an area that requires further study.

5.6.9. Limitations of OCT

The prognostic power of OCT relies on how well it can estimate the number of viable RGCs or their axons. Several factors can affect the accuracy of OCT parameters.

First, OCT is subject to segmentation error. Segmentation within the retina can be affected by structural abnormalities in the retina, tilted disc, optic nerve edema, axial length, refractive errors, media opacity or cyclotorsion (Chen and Kardon, 2016; Subei and Eggenberger, 2009). The measurement of RNFL or GCC thicknesses in these cases will be unreliable, precluding a significant portion of patients from having high quality OCT.

Second, OCT measures all structures within the segmented area. In patients with long-standing no light perception vision and marked optic atrophy where there was no measurable visual function, OCT still measured 45 μm of RNFL (Chan and Miller, 2007). OCT is inherently a structural measure, and therefore does not distinguish healthy from dysfunctional cellular structures and includes all RGC bodies, axons of dysfunctional cells, sheaths of dead axons, blood vessels and glial cells.

Thirdly, OCT devices compare measurements to a normative reference range and provide statistical abnormalities compared to the reference population. There is considerable variation in the amplitude and shape of the individual RNFL profiles, and functionally normal eyes can have RNFL measurements outside the range of normative data. This can lead to functionally normal eyes being classified as having 'abnormal' RNFL or GCC (Ghadiali et al., 2008). This variability will affect the sensitivity and specificity of any prognostic analysis of RNFL or GCC thinning, making studies with small sample sizes less reliable.

6. Post-decompression deterioration

Vision deteriorates in 1.5–12% of patients after decompression surgery (Cohen et al., 1985; Gnanalingham et al., 2005; Mortini et al., 2005; Powell, 1995; Salmi et al., 1982). Post-operative complications such as prolapse of the optic chiasm into an empty sella, intrasellar hematoma, ischemia, fracture of orbit, direct injury to the optic nerves, excessive fat packing and cerebral vasospasm are thought to be the main cause of early deterioration in vision (Barrow and Tindall, 1990; Chowdhury et al., 2014). Complication rates appear to be higher with large and invasive intracranial tumors (Sleep et al., 2003). Delayed visual deterioration usually indicates tumor recurrence or radiation necrosis in those who receive radiation therapy (Rivoal et al., 2000). .

7. Future directions and conclusion

The vision loss and recovery in chiasmal compression follows a complicated and highly variable path. Compression of the chiasm causes visual dysfunction via conduction block, demyelination and retrograde/anterograde degeneration. Theoretically, recovery takes place in three stages from the early post-operative phase where conduction begins to return, the intermediate phase where axons undergo remyelination and restoration of intracellular infrastructures, and the late phase where the neural network undergoes reorganization and collateral sprouting. Evidence suggests that localized chronic chiasmal compression evokes molecular and physiological changes in the entire visual system from the retina to the visual cortices. The neurobiology of this phenomenon requires much more investigation.

Prediction of post-decompression visual outcome is challenging because a compressed optic nerve consists of a mixed population of axons, each with variable functional and structural status and potential for recovery. Clinical variables, including patient age, duration of symptoms prior to surgery, tumor size, endocrine characteristics of tumors, optic disc pallor, pre-operative visual acuity and visual field loss have not been reported to predict visual recovery following decompression. More time-consuming and invasive modalities, such as electrophysiology, multifocal VEPs and neuroimaging, have also been trialled with variable results. A method which allows estimation of the quantity of viable RGCs and their functional capacity will give the best predictive power for visual outcome (Raz et al., 2015). At present, the OCT of RNFL and the GCC gives the most reliable measure of RGC damage (structural change), although it has its own limitations. The future challenge is to develop an *in vivo*, non-invasive and cost-effective test that can accurately measure the number and distribution of viable RGCs, while allowing distinction between reversible conduction block and permanent vision loss. Until then, a combination of clinical examination and multiple ancillary tests gives the best visual prognosis for patients undergoing chiasmal decompression.

Author contribution

Helen Danesh-Meyer 30%, Jinny Yoon 30%, Mitchell Lawlor 20%, Peter Savino 20%

Declaration of interest

None.

Acknowledgements

This work was supported by the NAR foundation Optic Nerve Research Fellowship. We would like to thank Ms Jessica Kirton, our medical illustrator, for her contribution to this manuscript. The authors have no conflicts of interest to declare.

Appendix A. Supplementary data

Supplementary data to this article can be found online at https://doi.org/10.1016/j.preteyeres.2019.06.001.

References

Abegg, M., Dysli, M., Wolf, S., Kowal, J., Dufour, P., Zinkernagel, M., 2014. Microcystic macular edema: retrograde maculopathy caused by optic neuropathy. Ophthalmology 121, 142–149.

Abrams, L.S., Scott, I.U., Spaeth, G.L., Quigley, H.A., Varma, R., 1994. Agreement among optometrists, ophthalmologists, and residents in evaluating the optic disc for glaucoma. Ophthalmology 101, 1662–1667.

Agrawal, D., Mahapatra, A.K., 2005. Visual outcome of blind eyes in pituitary apoplexy after transsphenoidal surgery: a series of 14 eyes. Surg. Neurol. 63, 42–46 discussion 46.

Almasieh, M., Wilson, A.M., Morquette, B., Cueva Vargas, J.L., Di Polo, A., 2012. The molecular basis of retinal ganglion cell death in glaucoma. Prog. Retin. Eye Res. 31, 152–181.

Anik, I., Anik, Y., Cabuk, B., Caklili, M., Pirhan, D., Ozturk, O., Cirak, M., Ceylan, S., 2018. Visual outcome of an endoscopic endonasal transsphenoidal approach in pituitary macroadenomas: quantitative assessment with diffusion tensor imaging early and long-term results. World Neurosurg. 112, e691–e701.

Anik, I., Anik, Y., Koc, K., Ceylan, S., Genc, H., Altintas, O., Ozdamar, D., Baykal Ceylan, D., 2011. Evaluation of early visual recovery in pituitary macroadenomas after endoscopic endonasal transphenoidal surgery: quantitative assessment with diffusion tensor imaging (DTI). Acta Neurochir. (Wien) 153, 831–842.

Astorga-Carballo, A., Serna-Ojeda, J.C., Camargo-Suarez, M.F., 2017. Chiasmal syndrome: clinical characteristics in patients attending an ophthalmological center. Saudi J. 31, 229–233.

Ayuk, J., McGregor, E.J., Mitchell, R.D., Gittoes, N.J., 2004. Acute management of pituitary apoplexy–surgery or conservative management? Clin. Endocrinol. 61, 747–752.

Barrow, D.L., Tindall, G.T., 1990. Loss of vision after transsphenoidal surgery. Neurosurgery 27, 60–68.

Barzaghi, L.R., Medone, M., Losa, M., Bianchi, S., Giovanelli, M., Mortini, P., 2012. Prognostic factors of visual field improvement after trans-sphenoidal approach for pituitary macroadenomas: review of the literature and analysis by quantitative method. Neurosurg. Rev. 35, 369–378 discussion 378-369.

Bergland, R., 1969. The arterial supply of the human optic chiasm. J. Neurosurg. 31, 327–334.

Berkelaar, M., Clarke, D.B., Wang, Y.C., Bray, G.M., Aguayo, A.J., 1994. Axotomy results in delayed death and apoptosis of retinal ganglion cells in adult rats. J. Neurosci. 14, 4368–4374.

Berkowitz, J.S., Balter, S., 1970. Colorimetric measurement of the optic disk. Am. J. Ophthalmol. 69, 385–386.

Bevan, J.S., Webster, J., Burke, C.W., Scanlon, M.F., 1992. Dopamine agonists and pituitary tumor shrinkage. Endocr. Rev. 13, 220–240.

Bianchi-Marzoli, S., Rizzo 3rd, J.F., Brancato, R., Lessell, S., 1995. Quantitative analysis of optic disc cupping in compressive optic neuropathy. Ophthalmology 102, 436–440.

Bostock, H., Sears, T.A., 1978. The internodal axon membrane: electrical excitability and continuous conduction in segmental demyelination. J. Physiol. (Lond.) 280, 273–301.

Brecelj, J., 1992. A VEP study of the visual pathway function in compressive lesions of the optic chiasm. Full-field versus half-field stimulation. Electroencephalogr. Clin. Neurophysiol. 84, 209–218.

Brecelj, J., Denislic, M., Skrbec, M., 1989. Visual evoked potential abnormalities in chiasmal lesions. Doc. Ophthalmol. 73, 139–148.

Brecelj, J., Štrucl, M., Škrbec, M., 1992. Visual evoked potentials in compressive lesions of the optic chiasm. Neuro Ophthalmol. 12, 207–214.

Campbell, W.W., 2008. Evaluation and management of peripheral nerve injury. Clin. Neurophysiol. 119, 1951–1965.

Carrim, Z.I., Reeks, G.A., Chohan, A.W., Dunn, L.T., Hadley, D.M., 2007. Predicting impairment of central vision from dimensions of the optic chiasm in patients with pituitary adenoma. Acta Neurochir. (Wien) 149, 255–260 discussion 260.

Cennamo, G., Auriemma, R.S., Cardone, D., Grasso, L.F., Velotti, N., Simeoli, C., Di Somma, C., Pivonello, R., Colao, A., de Crecchio, G., 2015. Evaluation of the retinal nerve fibre layer and ganglion cell complex thickness in pituitary macroadenomas without optic chiasmal compression. Eye 29, 797–802.

Chabot, J.D., Chakraborty, S., Imbarrato, G., Dehdashti, A.R., 2015. Evaluation of outcomes after endoscopic endonasal surgery for large and giant pituitary macroadenoma: a retrospective review of 39 consecutive patients. World Neurosurg. 84, 978–988.

Chacko, L.W., 1948. The laminar pattern of the lateral geniculate body in the primates. J. Neurol. Neurosurg. Psychiatry 11, 211–224.

Chan, C.K., Miller, N.R., 2007. Peripapillary nerve fiber layer thickness measured by optical coherence tomography in patients with no light perception from long-standing nonglaucomatous optic neuropathies. J. Neuro Ophthalmol. 27, 176–179.

Chen, C., Okera, S., Davies, P.E., Selva, D., Crompton, J.L., 2003. Craniopharyngioma: a review of long-term visual outcome. Clin. Exp. Ophthalmol. 31, 220–228.

Chen, J.J., Kardon, R.H., 2016. Avoiding clinical misinterpretation and artifacts of optical coherence tomography analysis of the optic nerve, retinal nerve fiber layer, and ganglion cell layer. J. Neuro Ophthalmol. 36, 417–438.

Chohan, M.O., Levin, A.M., Singh, R., Zhou, Z., Green, C.L., Kazam, J.J., Tsiouris, A.J., Anand, V.K., Schwartz, T.H., 2016. Three-dimensional volumetric measurements in defining endoscope-guided giant adenoma surgery outcomes. Pituitary 19, 311–321.

Chou, T.H., Park, K.K., Luo, X., Porciatti, V., 2013. Retrograde signaling in the optic nerve is necessary for electrical responsiveness of retinal ganglion cells. Investig. Ophthalmol. Vis. Sci. 54, 1236–1243.

Choudhry, O.J., Choudhry, A.J., Nunez, E.A., Eloy, J.A., Couldwell, W.T., Ciric, I.S., Liu, J.K., 2012. Pituitary tumor apoplexy in patients with Cushing's disease: endocrinologic and visual outcomes after transsphenoidal surgery. Pituitary 15, 428–435.

Chowdhury, T., Prabhakar, H., Bithal, P.K., Schaller, B., Dash, H.H., 2014. Immediate postoperative complications in transsphenoidal pituitary surgery: a prospective study. Saudi J. Anaesth. 8, 335–341.

Cioffi, G.A., 2005. Ischemic model of optic nerve injury. Trans. Am. Ophthalmol. Soc. 103, 592–613.

Clifford-Jones, R.E., Landon, D.N., McDonald, W.I., 1980. Remyelination during optic nerve compression. J. Neurol. Sci. 46, 239–243.

Clifford-Jones, R.E., McDonald, W.I., Landon, D.N., 1985. Chronic optic nerve compression. Exp. Stud. Brain 108, 241–262.

Cohen, A.R., Cooper, P.R., Kupersmith, M.J., Flamm, E.S., Ransohoff, J., 1985. Visual

recovery after transsphenoidal removal of pituitary adenomas. Neurosurgery 17, 446–452.
Corsello, S.M., Ubertini, G., Altomare, M., Lovicu, R.M., Migneco, M.G., Rota, C.A., Colosimo, C., 2003. Giant prolactinomas in men: efficacy of cabergoline treatment. Clin. Endocrinol. 58, 662–670.
Cottee, L.J., Daniel, C., Loh, W.S., Harrison, B.M., Burke, W., 2003. Remyelination and recovery of conduction in cat optic nerve after demyelination by pressure. Exp. Neurol. 184, 865–877.
Csillag, A., 2003. The organ of vision. In: Atlas of the Sensory Organs : Functional and Clinical Anatomy. Humana Press, Totowa, N.J., pp. 85–164.
Cui, Q., Ren, C., Sollars, P.J., Pickard, G.E., So, K.F., 2015. The injury resistant ability of melanopsin-expressing intrinsically photosensitive retinal ganglion cells. Neuroscience 284, 845–853.
Cunha, L.P., Oyamada, M.K., Monteiro, M.L., 2008. Pattern electroretinograms for the detection of neural loss in patients with permanent temporal visual field defect from chiasmal compression. Doc. Ophthalmol. 117, 223–232.
Cushing, H., Walker, C.B., 1915. Distortions of the visual fields in cases of brain tumour chiasmal lesions, with special reference to bitemporal hemianopsia. Brain 37, 341–400.
Danesh-Meyer, H.V., Carroll, S.C., Foroozan, R., Savino, P.J., Fan, J., Jiang, Y., Vander Hoorn, S., 2006a. Relationship between retinal nerve fiber layer and visual field sensitivity as measured by optical coherence tomography in chiasmal compression. Investig. Ophthalmol. Vis. Sci. 47, 4827–4835.
Danesh-Meyer, H.V., Carroll, S.C., Gaskin, B.J., Gao, A., Gamble, G.D., 2006b. Correlation of the multifocal visual evoked potential and standard automated perimetry in compressive optic neuropathies. Investig. Ophthalmol. Vis. Sci. 47, 1458–1463.
Danesh-Meyer, H.V., Papchenko, T., Savino, P.J., Law, A., Evans, J., Gamble, G.D., 2008. In vivo retinal nerve fiber layer thickness measured by optical coherence tomography predicts visual recovery after surgery for parachiasmal tumors. Investig. Ophthalmol. Vis. Sci. 49, 1879–1885.
Danesh-Meyer, H.V., Savino, P.J., Bilyk, J.R., Sergott, R.C., Kubis, K., 2001. Gaze-evoked amaurosis produced by intraorbital buckshot pellet. Ophthalmology 108, 201–206.
Danesh-Meyer, H.V., Wong, A., Papchenko, T., Matheos, K., Stylli, S., Nichols, A., Frampton, C., Daniell, M., Savino, P.J., Kaye, A.H., 2015. Optical coherence tomography predicts visual outcome for pituitary tumors. J. Clin. Neurosci. 22, 1098–1104.
Danesh-Meyer, H.V., Yap, J., Frampton, C., Savino, P.J., 2014. Differentiation of compressive from glaucomatous optic neuropathy with spectral-domain optical coherence tomography. Ophthalmology 121, 1516–1523.
Davies, E.W., 1970. Quantitative assessment of colour of the optic disc by a photographic method. Exp. Eye Res. 9, 106–113.
de Araujo, R.B., Oyamada, M.K., Zacharias, L.C., Cunha, L.P., Preti, R.C., Monteiro, M.L.R., 2017. Morphological and functional inner and outer retinal layer abnormalities in eyes with permanent temporal hemianopia from chiasmal compression. Front. Neurol. 8, 619.
Dekkers, O.M., de Keizer, R.J., Roelfsema, F., Vd Klaauw, A.A., Honkoop, P.J., van Dulken, H., Smit, J.W., Romijn, J.A., Pereira, A.M., 2007. Progressive improvement of impaired visual acuity during the first year after transsphenoidal surgery for nonfunctioning pituitary macroadenoma. Pituitary 10, 61–65.
Dutta, P., Gyurmey, T., Bansal, R., Pathak, A., Dhandapani, S., Rai, A., Bhansali, A., Mukherjee, K.K., 2016. Visual outcome in 2000 eyes following microscopic transsphenoidal surgery for pituitary adenomas: protracted blindness should not be a deterrent. Neurol. India 64, 1247–1253.
Dyck, P.J., Lais, A.C., Giannini, C., Engelstad, J.K., 1990. Structural alterations of nerve during cuff compression. Proc. Natl. Acad. Sci. U.S.A. 87, 9828–9832.
Ebersold, M.J., Quast, L.M., Laws Jr., E.R., Scheithauer, B., Randall, R.V., 1986. Long-term results in transsphenoidal removal of nonfunctioning pituitary adenomas. J. Neurosurg. 64, 713–719.
Eda, M., Saeki, N., Fujimoto, N., Sunami, K., 2002. Demonstration of the optic pathway in large pituitary adenoma on heavily T2 weighted MR images. Br. J. Neurosurg. 16, 21–29.
Farooq, K., Tayyaba Gul, M., Rashid, A., 2010. Pituitary macroadenomas; demographic, visual, and neuro-radiological patterns. Prof. Med. J. 17, 623–627.
Feinsod, M., Selhorst, J.B., Hoyt, W.F., Wilson, C.B., 1976. Monitoring optic nerve function during craniotomy. J. Neurosurg. 44, 29–31.
Findlay, G., McFadzean, R.M., Teasdale, G., 1983. Recovery of vision following treatment of pituitary tumours; application of a new system of assessment to patients treated by transsphenoidal operation. Acta Neurochir. (Wien) 68, 175–186.
Foroozan, R., 2003. Chiasmal syndromes. Curr. Opin. Ophthalmol. 14, 325–331.
Frisen, L., Sjostrand, J., Norrsell, K., Lindgren, S., 1976. Cyclic compression of the intracranial optic nerve: patterns of visual failure and recovery. J. Neurol. Neurosurg. Psychiatry 39, 1109–1113.
Funch, P.G., Faber, D.S., 1984. Measurement of myelin sheath resistances: implications for axonal conduction and pathophysiology. Science 225, 538–540.
Galetta, K.M., Calabresi, P.A., Frohman, E.M., Balcer, L.J., 2011. Optical coherence tomography (OCT): imaging the visual pathway as a model for neurodegeneration. Neurother. : J. Am. Soc. Exp. Neurother. 8, 117–132.
Gao, Y., Weng, C., Wang, X., 2013. Changes in nerve microcirculation following peripheral nerve compression. Neural Regen Res. 8, 1041–1047.
George, E.B., Glass, J.D., Griffin, J.W., 1995. Axotomy-induced axonal degeneration is mediated by calcium influx through ion-specific channels. J. Neurosci. 15, 6445–6452.
Ghadiali, Q., Hood, D.C., Lee, C., Manns, J., Llinas, A., Grover, L.K., Greenstein, V.C., Liebmann, J.M., Odel, J.G., Ritch, R., 2008. An analysis of normal variations in retinal nerve fiber layer thickness profiles measured with optical coherence tomography. J. Glaucoma 17, 333–340.
Ghaffarieh, A., Levin, L.A., 2012. Optic nerve disease and axon pathophysiology. Int. Rev. Neurobiol. 105, 1–17.
Glisson, C.C., 2014. Visual loss due to optic chiasm and retrochiasmal visual pathway lesions. Continuum: Lifelong Learn. Neurol. 20, 907–921.
Gnanalingham, K.K., Bhattacharjee, S., Pennington, R., Ng, J., Mendoza, N., 2005. The time course of visual field recovery following transphenoidal surgery for pituitary adenomas: predictive factors for a good outcome. J. Neurol. Neurosurg. Psychiatry 76, 415–419.
Goyal, J.L., Thangkhiew, L., Yadava, U., Arora, R., Jain, P., 2013. Evaluation of pattern ERG as a visual prognosticator in chiasmatic tumours. Clin. Exp. Ophthalmol. 41, 864–869.
Griessenauer, C.J., Raborn, J., Mortazavi, M.M., Tubbs, R.S., Cohen-Gadol, A.A., 2014. Relationship between the pituitary stalk angle in prefixed, normal, and postfixed optic chiasmata: an anatomic study with microsurgical application. Acta Neurochir. (Wien) 156, 147–151.
Grkovic, D., Davidovic, S., 2016. Prognostic factors for postoperative visual outcome in surgically treated suprasellar meningiomas. Med. Pregl. 69, 146–152.
Grosskreutz, J., Lin, C.S., Mogyoros, I., Burke, D., 2000. Ischaemic changes in refractoriness of human cutaneous afferents under threshold-clamp conditions. J. Physiol. 523, 807–815.
Gutin, P.H., Klemme, W.M., Lagger, R.L., MacKay, A.R., Pitts, L.H., Hosobuchi, Y., 1980. Management of the unresectable cystic craniopharyngioma by aspiration through an Ommaya reservoir drainage system. J. Neurosurg. 52, 36–40.
Gutowski, N.J., Heron, J.R., Scase, M.O., 1997. Early impairment of foveal magno- and parvocellular pathways in juxta chiasmal tumours. Vis. Res. 37, 1401–1408.
Hajiabadi, M., Samii, M., Fahlbusch, R., 2016. A preliminary study of the clinical application of optic pathway diffusion tensor tractography in suprasellar tumor surgery: preoperative, intraoperative, and postoperative assessment. J. Neurosurg. 125, 759–765.
Halliday, A.M., Halliday, L., Kriss, A., McDonald, W.I., Mushin, J., 1976. Abnormalities of the pattern evoked potential in compression of the anterior visual pathways. Trans. Ophthalmol. Soc. N. Z. 28, 37–40.
Hanke, J., Sabel, B.A., 2002. Anatomical correlations of intrinsic axon repair after partial optic nerve crush in rats.[Erratum appears in Ann Anat. 2006 Jul;188(4):376 Note: Sabel, BA [added]]. Ann. Anat. 184, 113–123.
Harrison, B.M., McDonald, W.I., 1977. Remyelination after transient experimental compression of the spinal cord. Ann. Neurol. 1, 542–551.
Hattar, S., Lucas, R.J., Mrosovsky, N., Thompson, S., Douglas, R.H., Hankins, M.W., Lem, J., Biel, M., Hofmann, F., Foster, R.G., Yau, K.W., 2003. Melanopsin and rod–cone photoreceptive systems account for all major accessory visual functions in mice. Nature 424, 75–81.
Hedges, T.R., 1969. Preservation of the upper nasal field in the chiasmal syndrome: an anatomic explanation. Trans. Am. Ophthalmol. Soc. 67, 131–141.
Higashiyama, T., Ichiyama, Y., Muraki, S., Nishida, Y., Ohji, M., 2016. Optical coherence tomography angiography of retinal perfusion in chiasmal compression. Ophthalmic Surg. Laser Imag. Retin. 47, 724–729.
Hirunpat, S., Tanomkiat, W., Sriprung, H., Chetpaophan, J., 2005. Optic tract edema: a highly specific magnetic resonance imaging finding for the diagnosis of craniopharyngiomas. Acta Radiol. 46, 419–423.
Hisanaga, S., Kakeda, S., Yamamoto, J., Watanabe, K., Moriya, J., Nagata, T., Fujino, Y., Kondo, H., Nishizawa, S., Korogi, Y., 2017. Pituitary macroadenoma and visual impairment: postoperative outcome prediction with contrast-enhanced FIESTA. AJNR Am. J. Neuroradiol. 38, 2067–2072.
Ho, R.W., Huang, H.M., Ho, J.T., 2015. The influence of pituitary adenoma size on vision and visual outcomes after trans-sphenoidal adenectomy: a report of 78 cases. J. Korean Neurosurg. Soc. 57, 23–31.
Hofer, S., Karaus, A., Frahm, J., 2010. Reconstruction and dissection of the entire human visual pathway using diffusion tensor MRI. Front. Neuroanat. 4, 15.
Hoffmann, M.B., Flechner, J.J., 2008. Slow pattern-reversal stimulation facilitates the assessment of retinal function with multifocal recordings. Clin. Neurophysiol. 119, 409–417.
Holder, G.E., 1978. The effects of chiasmal compression on the pattern visual evoked potential. Electroencephalogr. Clin. Neurophysiol. 45, 278–280.
Holder, G.E., 1987. Significance of abnormal pattern electroretinography in anterior visual pathway dysfunction. Br. J. Ophthalmol. 71, 166–171.
Holder, G.E., 1997. The pattern electroretinogram in anterior visual pathway dysfunction and its relationship to the pattern visual evoked potential: a personal clinical review of 743 eyes. Eye 11, 924–934.
Holder, G.E., 2004. Electrophysiological assessment of optic nerve disease. Eye 18, 1133–1143.
Horton, J.C., 1997. Wilbrand's knee of the primate optic chiasm is an artefact of monocular enucleation. Trans. Am. Ophthalmol. Soc. 95, 579–609.
Hoyt, W.F., 1970. Correlative functional anatomy of the optic chiasm —1969—. Neurosurgery 17, 189–208.
Hoyt, W.F., Luis, O., 1963. The primate chiasm. Details of visual fiber organization studied by silver impregnation techniques. Arch. Ophthalmol. 70, 69–85.
Hudson, H., Rissell, C., Gauderman, W.J., Feldon, S.E., 1991. Pituitary tumor volume as a predictor of postoperative visual field recovery. Quantitative analysis using automated static perimetry and computed tomography morphometry. J. Clin. Neuro Ophthalmol. 11, 280–283.
Ikeda, H., Yoshimoto, T., 1995. Visual disturbances in patients with pituitary adenoma. Acta Neurol. Scand. 92, 157–160.
Ikemoto, T., Tani, T., Taniguchi, S., Ikeuchi, M., Kimura, J., 2009. Effects of experimental focal compression on excitability of human median motor axons. Clin. Neurophysiol. 120, 342–347.
Ishikawa, H., Stein, D.M., Wollstein, G., Beaton, S., Fujimoto, J.G., Schuman, J.S., 2005.

Macular segmentation with optical coherence tomography. Investig. Ophthalmol. Vis. Sci. 46, 2012–2017.
Ito, Y.A., Di Polo, A., 2017. Mitochondrial dynamics, transport, and quality control: a bottleneck for retinal ganglion cell viability in optic neuropathies. Mitochondrion 36, 186–192.
Ivan, G., Szigeti-Csucs, N., Olah, M., Nagy, G.M., Goth, M.I., 2005. Treatment of pituitary tumors: dopamine agonists. Endocrine 28, 101–110.
Jacob, M., Raverot, G., Jouanneau, E., Borson-Chazot, F., Perrin, G., Rabilloud, M., Tilikete, C., Bernard, M., Vighetto, A., 2009. Predicting visual outcome after treatment of pituitary adenomas with optical coherence tomography. Am. J. Ophthalmol. 147, 64–70 e62.
Jacobson, S.G., Eames, R.A., McDonald, W.I., 1979. Optic nerve fibre lesions in adult cats: pattern of recovery of spatial vision. Exp. Brain Res. 36, 491–508.
Jain, N.S., Jain, S.V., Wang, X., Neely, A.J., Tahtali, M., Jain, S., Lueck, C.J., 2015. Visualization of nerve fiber orientations in the human optic chiasm using photomicrographic image analysis. Investig. Ophthalmol. Vis. Sci. 56, 6734–6739.
Jakobiec, F.A., Depot, M.J., Kennerdell, J.S., Shults, W.T., Anderson, R.L., Alper, M.E., Citrin, C.M., Housepian, E.M., Trokel, S.L., 1984. Combined clinical and computed tomographic diagnosis of orbital glioma and meningioma. Ophthalmology 91, 137–155.
Janaky, M., Benedek, G., 1992. Visual evoked potentials during the early phase of optic nerve compression in the orbital cavity. Doc. Ophthalmol. 81, 197–208.
Jayaraman, M., Ambika, S., Gandhi, R.A., Bassi, S.R., Ravi, P., Sen, P., 2010. Multifocal visual evoked potential recordings in compressive optic neuropathy secondary to pituitary adenoma. Doc. Ophthalmol. 121, 197–204.
Jeffery, G., 2001. Architecture of the optic chiasm and the mechanisms that sculpt its development. Physiol. Rev. 81, 1393–1414.
Johansson, C., Lindblom, B., 2009. The role of optical coherence tomography in the detection of pituitary adenoma. Acta Opthalmologica 87, 776–779.
Kamali, A., Hasan, K.M., Adapa, P., Razmandi, A., Keser, Z., Lincoln, J., Kramer, L.A., 2014. Distinguishing and quantification of the human visual pathways using high-spatial-resolution diffusion tensor tractography. Magn. Reson. Imaging 32, 796–803.
Kanamori, A., Catrinescu, M.M., Belisle, J.M., Costantino, S., Levin, L.A., 2012. Retrograde and Wallerian axonal degeneration occur synchronously after retinal ganglion cell axotomy. Am. J. Pathol. 181, 62–73.
Kanamori, A., Nakamura, M., Matsui, N., Nagai, A., Nakanishi, Y., Kusuhara, S., Yamada, Y., Negi, A., 2004. Optical coherence tomography detects characteristic retinal nerve fiber layer thickness corresponding to band atrophy of the optic discs. Ophthalmology 111, 2278–2283.
Karanjia, N., Jacobson, D.M., 1999. Compression of the prechiasmatic optic nerve produces a junctional scotoma. Am. J. Ophthalmol. 128, 256–258.
Kasputyte, R., Slatkeviciene, G., Liutkeviciene, R., Glebauskiene, B., Bernotas, G., Tamasauskas, A., 2013. Changes of visual functions in patients with pituitary adenoma. Medicina (Kaunas, Lithuania) 49, 132–137.
Kaufmann, D.I., Wray, S.H., Lorance, R., Woods, M., 1986. An analysis of the pathophysiology and the development of treatment strategies for compressive optic nerve lesions using pattern electroretinogram and visual evoked potential. Neurology 36 (Suppl. 1), 232.
Kawamura, N., Tabata, H., Sun-Wada, G.H., Wada, Y., 2010. Optic nerve compression and retinal degeneration in Tcirg1 mutant mice lacking the vacuolar-type H-ATPase a3 subunit. PLoS One 5, e12086.
Kayan, A., Earl, C.J., 1975. Compressive lesions of the optic nerves and chiasm. Pattern of recovery of vision following surgical treatment. Brain 98, 13–28.
Kerrison, J.B., Lynn, M.J., Baer, C.A., Newman, S.A., Biousse, V., Newman, N.J., 2000. Stages of improvement in visual fields after pituitary tumor resection. Am. J. Ophthalmol. 130, 813–820.
Kidd, D., 2014. The optic chiasm. Clin. Anat. 27, 1149–1158.
Kiernan, M.C., Kaji, R., 2013. Physiology and pathophysiology of myelinated nerve fibers. Handb. Clin. Neurol. 115, 43–53.
Kitao, A., Hirata, H., Morita, A., Yoshida, T., Uchida, A., 1997. Transient damage to the axonal transport system without Wallerian degeneration by acute nerve compression. Exp. Neurol. 147, 248–255.
Klauber, A., Rasmussen, P., Lindholm, J., 1978. Pituitary adenoma and visual function. The prognostic value of clinical, ophthalmological and neuroradiologic findings in 51 patients subjected to operation. Acta Ophthalmol. 56, 252–263.
Knapp, M.E., Flaharty, P.M., Sergott, R.C., Savino, P.J., Mazzoli, R.A., Flanagan, J.C., 1992. Gaze-induced amaurosis from central retinal artery compression. Ophthalmology 99, 238–240.
Knoferle, J., Koch, J.C., Ostendorf, T., Michel, U., Planchamp, V., Vutova, P., Tonges, L., Stadelmann, C., Bruck, W., Bahr, M., Lingor, P., 2010. Mechanisms of acute axonal degeneration in the optic nerve in vivo. Proc. Natl. Acad. Sci. U.S.A. 107, 6064–6069.
Kondo, Y., Ramaker, J.M., Radcliff, A.B., Baldassari, S., Mayer, J.A., Ver Hoeve, J.N., Zhang, C.L., Chiu, S.Y., Colello, R.J., Duncan, I.D., 2013. Spontaneous optic nerve compression in the osteopetrotic (op/op) mouse: a novel model of myelination failure. J. Neurosci. 33, 3514–3525.
Kosmorsky, G.S., Dupps Jr., W.J., Drake, R.L., 2008. Nonuniform pressure generation in the optic chiasm may explain bitemporal hemianopsia. Ophthalmology 115, 560–565.
Kupfer, C., Chumbley, L., Downer, J.C., 1967. Quantitative histology of optic nerve, optic tract and lateral geniculate nucleus of man. J. Anat. 101, 393–401.
Kuwabara, S., 2009. Carpal tunnel syndrome: demyelinative or ischemic conduction block? Clin. Neurophysiol. 120, 223–224.
La Morgia, C., Ross-Cisneros, F.N., Sadun, A.A., Hannibal, J., Munarini, A., Mantovani, V., Barboni, P., Cantalupo, G., Tozer, K.R., Sancisi, E., Salomao, S.R., Moraes, M.N., Moraes-Filho, M.N., Heegaard, S., Milea, D., Kjer, P., Montagna, P., Carelli, V., 2010. Melanopsin retinal ganglion cells are resistant to neurodegeneration in mitochondrial optic neuropathies. Brain 133, 2426–2438.
Lange, M., Pagotto, U., Hopfner, U., Ehrenreich, H., Oeckler, R., Sinowatz, F., Stalla, G.K., 1994. Endothelin expression in normal human anterior pituitaries and pituitary adenomas. J. Clin. Endocrinol. Metab. 79, 1864–1870.
Lao, Y., Gao, H., Zhong, Y., 1994. Vascular architecture of the human optic chiasma and bitemporal hemianopia. Chin. Med. Sci. J. 9, 38–44.
Lawlor, M., Quartilho, A., Bunce, C., Nathwani, N., Dowse, E., Kamal, D., Gazzard, G., 2017. Patients with normal tension glaucoma have relative sparing of the relative afferent pupillary defect compared to those with open angle glaucoma and elevated intraocular pressure. Investig. Ophthalmol. Vis. Sci. 58, 5237–5241.
Laws Jr., E.R., Trautmann, J.C., Hollenhorst Jr., R.W., 1977. Transsphenoidal decompression of the optic nerve and chiasm. Visual results in 62 patients. J. Neurosurg. 46, 717–722.
Lee, J., Kim, S.W., Kim, D.W., Shin, J.Y., Choi, M., Oh, M.C., Kim, S.M., Kim, E.H., Kim, S.H., Byeon, S.H., 2016. Predictive model for recovery of visual field after surgery of pituitary adenoma. J. Neuro Oncol. 130, 155–164.
Lee, J.H., Tobias, S., Kwon, J.T., Sade, B., Kosmorsky, G., 2006. Wilbrand's knee: does it exist? Surg. Neurol. 66, 11–17 discussion 17.
Lee, J.P., Park, I.W., Chung, Y.S., 2011. The volume of tumor mass and visual field defect in patients with pituitary macroadenoma. Korean J. Ophthalmol. 25, 37–41.
Lennerstrand, G., 1983. Visual recovery after treatment for pituitary adenoma. Acta Ophthalmol. 61, 1104–1117.
Lewis, T., Pickering, G.W., Rothschild, P., 1931. Centripetal paralysis arising out of arrested blood flow to the limb, including notes on a form of tingling. Heart 16, 1–32.
Lilja, Y., Gustafsson, O., Ljungberg, M., Starck, G., Lindblom, B., Skoglund, T., Bergquist, H., Jakobsson, K.E., Nilsson, D., 2017. Visual pathway impairment by pituitary adenomas: quantitative diagnostics by diffusion tensor imaging. J. Neurosurg. 127, 569–579.
Lin, H., Ingram, W.R., 1974a. Retrograde degeneration of primary optic fibers in the cat. Exp. Neurol. 44, 21–34.
Lin, H., Ingram, W.R., 1974b. Spatial and temporal distribution of axonal degeneration in the primary optic system of the cat. Exp. Neurol. 44, 10–20.
Loo, J.L., Tian, J., Miller, N.R., Subramanian, P.S., 2013. Use of optical coherence tomography in predicting post-treatment visual outcome in anterior visual pathway meningiomas. Br. J. Ophthalmol. 97, 1455–1458.
Lundstrom, M., Frisen, L., 1976. Atrophy of optic nerve fibres in compression of the chiasm. Degree and distribution of ophthalmoscopic changes. Acta Ophthalmol. 54, 623–640.
Lundstrom, M., Frisen, L., 1977. Atrophy of optic nerve fibres in compression of the chiasm. Prognostic implications. Acta Ophthalmol. 55, 208–216.
Maffei, L., Fiorentini, A., Bisti, S., Hollander, H., 1985. Pattern ERG in the monkey after section of the optic nerve. Exp. Brain Res. 59, 423–425.
Maitland, C.G., Aminoff, M.J., Kennard, C., Hoyt, W.F., 1982. Evoked potentials in the evaluation of visual field defects due to chiasmal or retrochiasmal lesions. Neurology 32, 986–991.
Marcus, M., Vitale, S., Calvert, P.C., Miller, N.R., 1991. Visual parameters in patients with pituitary adenoma before and after transsphenoidal surgery. Aust. N. Z. J. Ophthalmol. 19, 111–118.
Maxwell, W.L., Povlishock, J.T., Graham, D.L., 1997. A mechanistic analysis of nondisruptive axonal injury: a review. J. Neurotrauma 14, 419–440.
McDonald, W.I., 1982. The symptomatology of tumours of the anterior visual pathways. Can. J. Neurol. Sci. 9, 381–390.
McIlwaine, G.G., Carrim, Z.I., Lueck, C.J., Chrisp, T.M., 2005. A mechanical theory to account for bitemporal hemianopia from chiasmal compression. J. Neuro Ophthalmol. 25, 40–43.
Menorca, R.M.G., Fussell, T.S., Elfar, J.C., 2013. Nerve physiology: mechanisms of injury and recovery. Hand Clin. 29, 317–330.
Mikelberg, F.S., Drance, S.M., Schulzer, M., Yidegiligne, H.M., Weis, M.M., 1989. The normal human optic nerve. Axon count and axon diameter distribution. Ophthalmology 96, 1325–1328.
Mikelberg, F.S., Yidegiligne, H.M., 1993. Axonal loss in band atrophy of the optic nerve in craniopharyngioma: a quantitative analysis. Can. J. Ophthalmol. 28, 69–71.
Miller, N.R., Newman, N.J., Biousse, V., Kerrison, J.B., 2005. Walsh & Hoyt's Clinical Neuro-Ophthalmology, sixth ed. Lippincott Williams & Wilkins, Philadelphia.
Molitch, M.E., 2002. Medical management of prolactin-secreting pituitary adenomas. Pituitary 5, 55–65.
Moller-Goede, D.L., Brandle, M., Landau, K., Bernays, R.L., Schmid, C., 2011. Pituitary apoplexy: re-evaluation of risk factors for bleeding into pituitary adenomas and impact on outcome. Eur. J. Endocrinol. 164, 37–43.
Monteiro, M.L., Costa-Cunha, L.V., Cunha, L.P., Malta, R.F., 2010a. Correlation between macular and retinal nerve fibre layer Fourier-domain OCT measurements and visual field loss in chiasmal compression. Eye 24, 1382–1390.
Monteiro, M.L., Cunha, L.P., Costa-Cunha, L.V., Maia Jr., O.O., Oyamada, M.K., 2009. Relationship between optical coherence tomography, pattern electroretinogram and automated perimetry in eyes with temporal hemianopia from chiasmal compression. Investig. Ophthalmol. Vis. Sci. 50, 3535–3541.
Monteiro, M.L., Hokazono, K., Cunha, L.P., Oyamada, M.K., 2012. Multifocal pattern electroretinography for the detection of neural loss in eyes with permanent temporal hemianopia or quadrantanopia from chiasmal compression. Br. J. Ophthalmol. 96, 104–109.
Monteiro, M.L., Hokazono, K., Cunha, L.P., Oyamada, M.K., 2013. Correlation between multifocal pattern electroretinography and Fourier-domain OCT in eyes with temporal hemianopia from chiasmal compression. Graefes Arch. Clin. Exp. Ophthalmol. 251, 903–915.
Monteiro, M.L., Hokazono, K., Fernandes, D.B., Costa-Cunha, L.V., Sousa, R.M., Raza, A.S., Wang, D.L., Hood, D.C., 2014. Evaluation of inner retinal layers in eyes with

temporal hemianopic visual loss from chiasmal compression using optical coherence tomography. Investig. Ophthalmol. Vis. Sci. 55, 3328–3336.
Monteiro, M.L., Leal, B.C., Rosa, A.A., Bronstein, M.D., 2004. Optical coherence tomography analysis of axonal loss in band atrophy of the optic nerve. Br. J. Ophthalmol. 88, 896–899.
Monteiro, M.L., Medeiros, F.A., Ostroscki, M.R., 2003. Quantitative analysis of axonal loss in band atrophy of the optic nerve using scanning laser polarimetry. Br. J. Ophthalmol. 87, 32–37.
Monteiro, M.L., Zambon, B.K., Cunha, L.P., 2010b. Predictive factors for the development of visual loss in patients with pituitary macroadenomas and for visual recovery after optic pathway decompression. Can. J. Ophthalmol. 45, 404–408.
Monteiro, M.L.R., 2018. Macular ganglion cell complex reduction preceding visual field loss in a patient with chiasmal compression with a 21-month follow-up. J. Neuro Ophthalmol. 38, 124–127.
Moon, C.H., Hwang, S.C., Kim, B.T., Ohn, Y.H., Park, T.K., 2011a. Visual prognostic value of optical coherence tomography and photopic negative response in chiasmal compression. Investig. Ophthalmol. Vis. Sci. 52, 8527–8533.
Moon, C.H., Hwang, S.C., Ohn, Y.H., Park, T.K., 2011b. The time course of visual field recovery and changes of retinal ganglion cells after optic chiasmal decompression. Investig. Ophthalmol. Vis. Sci. 52, 7966–7973.
Moraes, A.B., Silva, C.M., Vieira Neto, L., Gadelha, M.R., 2013. Giant prolactinomas: the therapeutic approach. Clin. Endocrinol. 79, 447–456.
Morgan, J.E., 2002. Retinal ganglion cell shrinkage in glaucoma. J. Glaucoma 11, 365–370.
Morgan, J.E., 2004. Circulation and axonal transport in the optic nerve. Eye 18, 1089–1095.
Morgan, W.H., Yu, D.Y., Cooper, R.L., Alder, V.A., Cringle, S.J., Constable, I.J., 1995. The influence of cerebrospinal fluid pressure on the lamina cribrosa tissue pressure gradient. Investig. Ophthalmol. Vis. Sci. 36, 1163–1172.
Mortini, P., Losa, M., Barzaghi, R., Boari, N., Giovanelli, M., 2005. Results of transsphenoidal surgery in a large series of patients with pituitary adenoma. Neurosurgery 56, 1222–1233 discussion 1233.
Mou, C., Han, T., Zhao, H., Wang, S., Qu, Y., 2009. Clinical features and immunohistochemical changes of pituitary apoplexy. J. Clin. Neurosci. 16, 64–68.
Moura, F.C., Costa-Cunha, L.V., Malta, R.F., Monteiro, M.L., 2010. Relationship between visual field sensitivity loss and quadrantic macular thickness measured with Stratus-Optical coherence tomography in patients with chiasmal syndrome. Arq. Bras. Oftalmol. 73, 409–413.
Moura, F.C., Medeiros, F.A., Monteiro, M.L., 2007. Evaluation of macular thickness measurements for detection of band atrophy of the optic nerve using optical coherence tomography. Ophthalmology 114, 175–181.
Muskens, I.S., Zamanipoor Najafabadi, A.H., Briceno, V., Lamba, N., Senders, J.T., van Furth, W.R., Verstegen, M.J.T., Smith, T.R.S., Mekary, R.A., Eenhorst, C.A.E., Broekman, M.L.D., 2017. Visual outcomes after endoscopic endonasal pituitary adenoma resection: a systematic review and meta-analysis. Pituitary 20, 539–552.
Muthukumar, N., Rossette, D., Soundaram, M., Senthilbabu, S., Badrinarayanan, T., 2008. Blindness following pituitary apoplexy: timing of surgery and neuro-ophthalmic outcome. J. Clin. Neurosci. 15, 873–879.
Nagahata, M., Hosoya, T., Kayama, T., Yamaguchi, K., 1998. Edema along the optic tract: a useful MR finding for the diagnosis of craniopharyngiomas. AJNR Am. J. Neuroradiol. 19, 1753–1757.
Neveu, M.M., Holder, G.E., Ragge, N.K., Sloper, J.J., Collin, J.R., Jeffery, G., 2006. Early midline interactions are important in mouse optic chiasm formation but are not critical in man: a significant distinction between man and mouse. Eur. J. Neurosci. 23, 3034–3042.
Newman, N.M., Tornambe, P.E., Corbett, J.J., 1982. Ophthalmoscopy of the retinal nerve fiber layer. Use in detection of neurologic disease. Arch. Neurol. 39, 226–233.
O'Connell, J.E., 1973. The anatomy of the optic chiasma and heteronymous hemianopia. J. Neurol. Neurosurg. Psychiatry 36, 710–723.
Ochs, S., Hollingsworth, D., 1971. Dependence of fast axoplasmic transport in nerve on oxidative metabolism. J. Neurochem. 18, 107–114.
Ogra, S., Nichols, A.D., Stylli, S., Kaye, A.H., Savino, P.J., Danesh-Meyer, H.V., 2014. Visual acuity and pattern of visual field loss at presentation in pituitary adenoma. J. Clin. Neurosci. 21, 735–740.
Ohkubo, S., Higashide, T., Takeda, H., Murotani, E., Hayashi, Y., Sugiyama, K., 2012. Relationship between macular ganglion cell complex parameters and visual field parameters after tumor resection in chiasmal compression. Jpn. J. Ophthalmol. 56, 68–75.
Otto, C.S., Coppit, G.L., Mazzoli, R.A., Eusterman, V.D., Nixon, K.L., Ainbinder, D.J., Raymond, W.R.t., Krolicki, T.J., Grazko, M.A., Hansen, E.A., 2003. Gaze-evoked Amaurosis: a Report of Five Cases. vol. 1. pp. 322–326.
Ouyang, H., Sun, W., Fu, Y., Li, J., Cheng, J.X., Nauman, E., Shi, R., 2010. Compression induces acute demyelination and potassium channel exposure in spinal cord. J. Neurotrauma 27, 1109–1120.
Parent, A.D., 1990. Visual recovery after blindness from pituitary apoplexy. Can. J. Neurol. Sci. 17, 88–91.
Park, H.H., Oh, M.C., Kim, E.H., Kim, C.Y., Kim, S.H., Lee, K.S., Chang, J.H., 2015. Use of optical coherence tomography to predict visual outcome in parachiasmal meningioma. J. Neurosurg. 123, 1489–1499.
Parmar, D.N., Sofat, A., Bowman, R., Bartlett, J.R., Holder, G.E., 2000. Visual prognostic value of the pattern electroretinogram in chiasmal compression. Br. J. Ophthalmol. 84, 1024–1026.
Paul, D.A., Gaffin-Cahn, E., Hintz, E.B., Adeclat, G.J., Zhu, T., Williams, Z.R., Vates, G.E., Mahon, B.Z., 2014. White matter changes linked to visual recovery after nerve decompression. Sci. Transl. Med. 6, 266ra173.
Peter, M., De Tribolet, N., 1995. Visual outcome after transsphenoidal surgery for pituitary adenomas. Br. J. Neurosurg. 9, 151–157.
Phal, P.M., Steward, C., Nichols, A.D., Kokkinos, C., Desmond, P.M., Danesh-Meyer, H., Sufaro, Y.Z., Kaye, A.H., Moffat, B.A., 2016. Assessment of optic pathway structure and function in patients with compression of the optic chiasm: a correlation with optical coherence tomography. Investig. Ophthalmol. Vis. Sci. 57, 3884–3890.
Piette, S.D., Sergott, R.C., 2006. Pathological optic-disc cupping. Curr. Opin. Ophthalmol. 17, 1–6.
Pizzorusso, T., Fagiolini, M., Porciatti, V., Maffei, L., 1997. Temporal aspects of contrast visual evoked potentials in the pigmented rat: effect of dark rearing. Vis. Res. 37, 389–395.
Poon, A., McNeill, P., Harper, A., O'Day, J., 1995. Patterns of visual loss associated with pituitary macroadenomas. Aust. N. Z. J. Ophthalmol. 23, 107–115.
Porciatti, V., Ciavarella, P., Ghiggi, M.R., D'Angelo, V., Padovano, S., Grifa, M., Moretti, G., 1999. Losses of hemifield contrast sensitivity in patients with pituitary adenoma and normal visual acuity and visual field. Clin. Neurophysiol. 110, 876–886.
Portney, G.L., Roth, A.M., 1977. Optic cupping caused by an intracranial aneurysm. Am. J. Ophthalmol. 84, 98–103.
Powell, M., 1995. Recovery of vision following transsphenoidal surgery for pituitary adenomas. Br. J. Neurosurg. 9, 367–373.
Prieto, R., Pascual, J.M., Barrios, L., 2015. Optic chiasm distortions caused by craniopharyngiomas: clinical and magnetic resonance imaging correlation and influence on visual outcome. World Neurosurg. 83, 500–529.
Pullan, P.T., Carroll, W.M., Chakera, T.M., Khangure, M.S., Vaughan, R.J., 1985. Management of extra-sellar pituitary tumours with bromocriptine: comparison of prolactin secreting and non-functioning tumours using half-field visual evoked potentials and computerised tomography. Aust. N. Z. J. Med. 15, 203–208.
Qiao, N., Zhang, Y., Ye, Z., Shen, M., Shou, X., Wang, Y., Li, S., Wang, M., Zhao, Y., 2015. Comparison of multifocal visual evoked potential, static automated perimetry, and optical coherence tomography findings for assessing visual pathways in patients with pituitary adenomas. Pituitary 18, 598–603.
Qu, Y., Wang, Y.X., Xu, L., Zhang, L., Zhang, J., Zhang, J., Wang, L., Yang, L., Yang, A., Wang, J., Jonas, J.B., 2011. Glaucoma-like optic neuropathy in patients with intracranial tumours. Acta Ophthalmol. 89, e428–433.
Raff, M.C., Whitmore, A.V., Finn, J.T., 2002. Axonal self-destruction and neurodegeneration. Science 296, 868–871.
Randeva, H.S., Schoebel, J., Byrne, J., Esiri, M., Adams, C.B., Wass, J.A., 1999. Classical pituitary apoplexy: clinical features, management and outcome. Clin. Endocrinol. 51, 181–188.
Raz, N., Bick, A.S., Klistorner, A., Spektor, S., Reich, D.S., Ben-Hur, T., Levin, N., 2015. Physiological correlates and predictors of functional recovery after chiasmal decompression. J. Neuro Ophthalmol. 35, 348–352.
Reid, R.L., Quigley, M.E., Yen, S.S., 1985. Pituitary apoplexy. A review. Arch. Neurol. 42, 712–719.
Ren, R., Jonas, J.B., Tian, G., Zhen, Y., Ma, K., Li, S., Wang, H., Li, B., Zhang, X., Wang, N., 2010. Cerebrospinal fluid pressure in glaucoma: a prospective study. Ophthalmology 117, 259–266.
Ritchie, J.M., Rogart, R.B., 1977. Density of sodium channels in mammalian myelinated nerve fibers and nature of the axonal membrane under the myelin sheath. Proc. Natl. Acad. Sci. U.S.A. 74, 211–215.
Rivoal, O., Brezin, A.P., Feldman-Billard, S., Luton, J.P., 2000. Goldmann perimetry in acromegaly: a survey of 307 cases from 1951 through 1996. Ophthalmology 107, 991–997.
Roebroeck, A., Galuske, R., Formisano, E., Chiry, O., Bratzke, H., Ronen, I., Kim, D.S., Goebel, R., 2008. High-resolution diffusion tensor imaging and tractography of the human optic chiasm at 9.4 T. Neuroimage 39, 157–168.
Romano, M.R., Angi, M., Romano, V., Marticorena, J., Romano, F., 2010. Early unilateral macular sensitivity changes in microperimetry in a case of pituitary adenoma. Int. Ophthalmol. 30, 709–711.
Ruther, K., Ehlich, P., Philipp, A., Eckstein, A., Zrenner, E., 1998. Prognostic value of the pattern electroretinogram in cases of tumors affecting the optic pathway. Graefes Arch. Clin. Exp. Ophthalmol. 236, 259–263.
Sadowski, B., Altenmüller, E., Zrenner, E., 1995. Electrophysiological and psychophysical examination in patients with optic nerve compression. Neuro Ophthalmol. 15, 223–231.
Saeki, N., Murai, H., Kubota, M., Fujimoto, N., 2001. Oedema along the optic tracts due to pituitary metastasis. Br. J. Neurosurg. 15, 523–526.
Saeki, N., Uchino, Y., Murai, H., Kubota, M., Isobe, K., Uno, T., Sunami, K., Yamaura, A., 2003. MR imaging study of edema-like change along the optic tract in patients with pituitary region tumors. AJNR Am. J. Neuroradiol. 24, 336–342.
Salmi, J., Grahne, B., Valtonen, S., Pelkonen, R., 1982. Recurrence of chromophobe pituitary adenomas after operation and postoperative radiotherapy. Acta Neurol. Scand. 66, 681–689.
Salvatore, S., Vingolo, E.M., 2010. Endothelin-1 role in human eye: a review. J. Ophthalmol. 2010, 354645.
Sanno, N., Oyama, K., Tahara, S., Teramoto, A., Kato, Y., 2003. A survey of pituitary incidentaloma in Japan. Eur. J. Endocrinol. 149, 123–127.
Sarlls, J.E., Pierpaoli, C., 2009. In vivo diffusion tensor imaging of the human optic chiasm at sub-millimeter resolution. Neuroimage 47, 1244–1251.
Schiefer, U., Isbert, M., Mikolaschek, E., Mildenberger, I., Krapp, E., Schiller, J., Thanos, S., Hart, W., 2004. Distribution of scotoma pattern related to chiasmal lesions with special reference to anterior junction syndrome. Graefes Arch. Clin. Exp. Ophthalmol. 242, 468–477.
Schlechte, J.A., 2007. Long-term management of prolactinomas. J. Clin. Endocrinol. Metab. 92, 2861–2865.
Schmalisch, K., Milian, M., Schimitzek, T., Lagreze, W.A., Honegger, J., 2012. Predictors for visual dysfunction in nonfunctioning pituitary adenomas - implications for

neurosurgical management. Clin. Endocrinol. 77, 728–734.
Schultz, V., van der Meer, F., Wrzos, C., Scheidt, U., Bahn, E., Stadelmann, C., Bruck, W., Junker, A., 2017. Acutely damaged axons are remyelinated in multiple sclerosis and experimental models of demyelination. Glia 65, 1350–1360.
Schwartz, B., Reinstein, N.M., Lieberman, D.M., 1973. Pallor of the optic disc. Quantitative photographic evaluation. Arch. Ophthalmol. 89, 278–286.
Seidl, A.H., 2014. Regulation of conduction time along axons. Neuroscience 276, 126–134.
Seuk, J.W., Kim, C.H., Yang, M.S., Cheong, J.H., Kim, J.M., 2011. Visual outcome after transsphenoidal surgery in patients with pituitary apoplexy. J. Korean Neurosurg. Soc. 49, 339–344.
Sheth, S., Branstetter, B.F.t., Escott, E.J., 2009. Appearance of normal cranial nerves on steady-state free precession MR images. Radiographics 29, 1045–1055.
Shimon, I., Benbassat, C., Hadani, M., 2007. Effectiveness of long-term cabergoline treatment for giant prolactinoma: study of 12 men. Eur. J. Endocrinol. 156, 225–231.
Siliprandi, R., Bucci, M.G., Canella, R., Carmignoto, G., 1988. Flash and pattern electroretinograms during and after acute intraocular pressure elevation in cats. Investig. Ophthalmol. Vis. Sci. 29, 558–565.
Sleep, T.J., Hodgkins, P.R., Honeybul, S., Neil-Dwyer, G., Lang, D., Evans, B., 2003. Visual function following neurosurgical optic nerve decompression for compressive optic neuropathy. Eye 17, 571–578.
Smith, K.J., Blakemore, W.F., McDonald, W.I., 1981. The restoration of conduction by central remyelination. Brain 104, 383–404.
Song, S.K., Sun, S.W., Ju, W.K., Lin, S.J., Cross, A.H., Neufeld, A.H., 2003. Diffusion tensor imaging detects and differentiates axon and myelin degeneration in mouse optic nerve after retinal ischemia. Neuroimage 20, 1714–1722.
Song, S.K., Yoshino, J., Le, T.Q., Lin, S.J., Sun, S.W., Cross, A.H., Armstrong, R.C., 2005. Demyelination increases radial diffusivity in corpus callosum of mouse brain. Neuroimage 26, 132–140.
Sorensen, N., 1979. The pallor of the optic disc. A quantitative photographic assessment by purple filter. Acta Ophthalmol. 57, 718–724.
Sousa, R.M., Oyamada, M.K., Cunha, L.P., Monteiro, M.L.R., 2017. Multifocal visual evoked potential in eyes with temporal hemianopia from chiasmal compression: correlation with standard automated perimetry and OCT findings. Investig. Ophthalmol. Vis. Sci. 58, 4436–4449.
Spry, P.G., Spencer, I.C., Sparrow, J.M., Peters, T.J., Brookes, S.T., Gray, S., Baker, I., Furber, J.E., Easty, D.L., 1999. The Bristol Shared Care Glaucoma Study: reliability of community optometric and hospital eye service test measures. Br. J. Ophthalmol. 83, 707–712.
Staempfli, P., Rienmueller, A., Reischauer, C., Valavanis, A., Boesiger, P., Kollias, S., 2007. Reconstruction of the human visual system based on DTI fiber tracking. J. Magn. Reson. Imaging 26, 886–893.
Stark, K.L., Kaufman, B., Lee, B.C., Primack, J., Tychsen, L., 1999. Visual recovery after a year of craniopharyngioma-related amaurosis: report of a nine-year-old child and a review of pathophysiologic mechanisms. J. AAPOS: Am. Assoc. Pediatr. Ophthalmol. Strabismus 3, 366–371.
Strucl, M., Brecelj, J., Hawlina, M., 1997. Visual evoked potential abnormalities in compressive chiasmal lesions: the relevance of central visual field defects. Neuro Ophthalmol. 17, 91–100.
Subei, A.M., Eggenberger, E.R., 2009. Optical coherence tomography: another useful tool in a neuro-ophthalmologist's armamentarium. Curr. Opin. Ophthalmol. 20, 462–466.
Sullivan, L.J., O'Day, J., McNeill, P., 1991. Visual outcomes of pituitary adenoma surgery. St. Vincent's Hospital 1968-1987. J. Clin. Neuro Ophthalmol. 11, 262–267.
Sun, M., Zhang, Z.-Q., Ma, C.-Y., Chen, S.-H., Chen, X.-J., 2017a. Predictive factors of visual function recovery after pituitary adenoma resection: a literature review and Meta-analysis. Int. J. Ophthalmol. 10, 1742–1750.
Sun, M., Zhang, Z., Ma, C., Chen, S., Chen, X., 2017b. Quantitative analysis of retinal layers on three-dimensional spectral-domain optical coherence tomography for pituitary adenoma. PLoS One 12, e0179532.
Takeda, N., Fujita, K., Katayama, S., Akutu, N., Hayashi, S., Kohmura, E., 2010. Effect of transsphenoidal surgery on decreased visual acuity caused by pituitary apoplexy. Pituitary 13, 154–159.
Takihara, Y., Inatani, M., Hayashi, H., Adachi, N., Iwao, K., Inoue, T., Iwao, M., Tanihara, H., 2011. Dynamic imaging of axonal transport in living retinal ganglion cells in vitro. Investig. Ophthalmol. Vis. Sci. 52, 3039–3045.
Tan, O., Chopra, V., Lu, A.T., Schuman, J.S., Ishikawa, H., Wollstein, G., Varma, R., Huang, D., 2009. Detection of macular ganglion cell loss in glaucoma by Fourier-domain optical coherence tomography. Ophthalmology 116, 2305–2314 e2301-2302.
Tasan, E., Hanimoglu, H., Turgut, S., Ilhan, M.M., Evran, S., Kaynar, M.Y., 2015. Rapid improvement in visual loss with cabergoline treatment in a giant prolactinoma case: 5 years survey. Neuroendocrinol. Lett. 36, 28–30.
Tieger, M.G., Hedges 3rd, T.R., Ho, J., Erlich-Malona, N.K., Vuong, L.N., Athappilly, G.K., Mendoza-Santiesteban, C.E., 2017. Ganglion cell complex loss in chiasmal compression by brain tumors. J. Neuro Ophthalmol. 37, 7–12.
Tokumaru, A.M., Sakata, I., Terada, H., Kosuda, S., Nawashiro, H., Yoshii, M., 2006. Optic nerve hyperintensity on T2-weighted images among patients with pituitary macroadenoma: correlation with visual impairment. AJNR Am. J. Neuroradiol. 27, 250–254.
Trobe, J.D., Tao, A.H., Schuster, J.J., 1984. Perichiasmal tumors: diagnostic and prognostic features. Neurosurgery 15, 391–399.
Unsold, R., Hoyt, W.F., 1980. Band atrophy of the optic nerve. The histology of temporal hemianopsia. Arch. Ophthalmol. 98, 1637–1638.
Ventura, L.M., Venzara 3rd, F.X., Porciatti, V., 2009. Reversible dysfunction of retinal ganglion cells in non-secreting pituitary tumors. Doc. Ophthalmol. 118, 155–162.
Wang, H., Sun, W., Fu, Z., Si, Z., Zhu, Y., Zhai, G., Zhao, G., Xu, S., Pang, Q., 2008. The pattern of visual impairment in patients with pituitary adenoma. J. Int. Med. Res. 36, 1064–1069.
Wang, X., Neely, A.J., McIlwaine, G.G., Lueck, C.J., 2014a. Multi-scale analysis of optic chiasmal compression by finite element modelling. J. Biomech. 47, 2292–2299.
Wang, X., Neely, A.J., McIlwaine, G.G., Lueck, C.J., 2016. Biomechanics of chiasmal compression: sensitivity of the mechanical behaviors of nerve fibers to variations in material property and geometry. Int. J. Comput. Methods Eng. Sci. Mech. 17, 165–171.
Wang, X., Neely, A.J., McIlwaine, G.G., Tahtali, M., Lillicrap, T.P., Lueck, C.J., 2014b. Finite element modeling of optic chiasmal compression. J. Neuro Ophthalmol. 34, 324–330.
Watanabe, K., Kakeda, S., Yamamoto, J., Watanabe, R., Nishimura, J., Ohnari, N., Nishizawa, S., Korogi, Y., 2012. Delineation of optic nerves and chiasm in close proximity to large suprasellar tumors with contrast-enhanced FIESTA MR imaging. Radiology 264, 852–858.
Waxman, S.G., Swadlow, H.A., 1977. The conduction properties of axons in central white matter. Prog. Neurobiol. 8, 297–324.
Wilbrand, H.L., 1926. Schema des Verlaufs der Sehnervenfasern durch das Chiasma. Ophthalmologica 59, 135–144.
Woodhouse, N.J., Khouqueer, F., Sieck, J.O., 1981. Prolactinomas and optic nerve compression: disappearance of suprasellar extension and visual recovery after two weeks bromocriptine treatment. Horm. Res. 14, 141–147.
Yates, S.K., Hurst, L.N., Brown, W.F., 1981. The pathogenesis of pneumatic tourniquet paralysis in man. J. Neurol. Neurosurg. Psychiatry 44, 759–767.
Yoneoka, Y., Hatase, T., Watanabe, N., Jinguji, S., Okada, M., Takagi, M., Fujii, Y., 2015. Early morphological recovery of the optic chiasm is associated with excellent visual outcome in patients with compressive chiasmal syndrome caused by pituitary tumors. Neurol. Res. 37, 1–8.
Yum, H.R., Park, S.H., Park, H.Y., Shin, S.Y., 2016. Macular ganglion cell analysis determined by cirrus HD optical coherence tomography for early detecting chiasmal compression. PLoS One 11, e0153064.
Zaidi, H.A., Cote, D.J., Burke, W.T., Castlen, J.P., Bi, W.L., Laws Jr., E.R., Dunn, I.F., 2016. Time course of symptomatic recovery after endoscopic transsphenoidal surgery for pituitary adenoma apoplexy in the modern era. World Neurosurg. 96, 434–439.
Zhang, J., Zhang, S., Song, Y., Zhu, C., He, M., Ren, Q., Shan, B., Wang, Z., Zeng, Y., Xu, J., 2017. Predictive value of preoperative retinal nerve fiber layer thickness for postoperative visual recovery in patients with chiasmal compression. Oncotarget 8, 59148–59155.
Zhang, X., Sun, P., Wang, J., Wang, Q., Song, S.K., 2011. Diffusion tensor imaging detects retinal ganglion cell axon damage in the mouse model of optic nerve crush. Investig. Ophthalmol. Vis. Sci. 52, 7001–7006.